NASA/TM—2013-217720

Solar Simulation for the CREST Preflight Thermal-Vacuum Test at B-2

Robert A. Ziemke
Glenn Research Center, Cleveland, Ohio

March 2013

NASA STI Program . . . in Profile

Since its founding, NASA has been dedicated to the advancement of aeronautics and space science. The NASA Scientific and Technical Information (STI) program plays a key part in helping NASA maintain this important role.

The NASA STI Program operates under the auspices of the Agency Chief Information Officer. It collects, organizes, provides for archiving, and disseminates NASA's STI. The NASA STI program provides access to the NASA Aeronautics and Space Database and its public interface, the NASA Technical Reports Server, thus providing one of the largest collections of aeronautical and space science STI in the world. Results are published in both non-NASA channels and by NASA in the NASA STI Report Series, which includes the following report types:

- TECHNICAL PUBLICATION. Reports of completed research or a major significant phase of research that present the results of NASA programs and include extensive data or theoretical analysis. Includes compilations of significant scientific and technical data and information deemed to be of continuing reference value. NASA counterpart of peer-reviewed formal professional papers but has less stringent limitations on manuscript length and extent of graphic presentations.

- TECHNICAL MEMORANDUM. Scientific and technical findings that are preliminary or of specialized interest, e.g., quick release reports, working papers, and bibliographies that contain minimal annotation. Does not contain extensive analysis.

- CONTRACTOR REPORT. Scientific and technical findings by NASA-sponsored contractors and grantees.

- CONFERENCE PUBLICATION. Collected papers from scientific and technical conferences, symposia, seminars, or other meetings sponsored or cosponsored by NASA.

- SPECIAL PUBLICATION. Scientific, technical, or historical information from NASA programs, projects, and missions, often concerned with subjects having substantial public interest.

- TECHNICAL TRANSLATION. English-language translations of foreign scientific and technical material pertinent to NASA's mission.

Specialized services also include creating custom thesauri, building customized databases, organizing and publishing research results.

For more information about the NASA STI program, see the following:

- Access the NASA STI program home page at *http://www.sti.nasa.gov*

- E-mail your question to *help@sti.nasa.gov*

- Fax your question to the NASA STI Information Desk at 443–757–5803

- Phone the NASA STI Information Desk at 443–757–5802

- Write to:
  STI Information Desk
  NASA Center for AeroSpace Information
  7115 Standard Drive
  Hanover, MD 21076–1320

NASA/TM—2013-217720

Solar Simulation for the CREST Preflight Thermal-Vacuum Test at B-2

Robert A. Ziemke
Glenn Research Center, Cleveland, Ohio

Prepared for the
Aerospace Testing Seminar (ATS)
sponsored by The Aerospace Corporation
Los Angeles, California, October 16–18, 2012

National Aeronautics and
Space Administration

Glenn Research Center
Cleveland, Ohio 44135

March 2013

Level of Review: This material has been technically reviewed by technical management.

Available from

NASA Center for Aerospace Information
7115 Standard Drive
Hanover, MD 21076–1320

National Technical Information Service
5301 Shawnee Road
Alexandria, VA 22312

Available electronically at http://www.sti.nasa.gov

Contents

Solar Simulation for the CREST Preflight Thermal-Vacuum Test at B-2

Robert A. Ziemke
National Aeronautics and Space Administration
Glenn Research Center
Cleveland, Ohio 44135

Abstract

In June 2011, the multi-university sponsored Cosmic Ray Electron Synchrotron Telescope (CREST) has undergone thermal-vacuum qualification testing at the NASA Glenn Research Center (GRC), Plum Brook Station, Sandusky, Ohio. The testing was performed in the B-2 Space Propulsion Facility vacuum chamber. The CREST was later flown over the Antarctic region as the payload of a stratospheric balloon. Solar simulation was provided by a system of planar infrared lamp arrays specifically designed for CREST. The lamp arrays, in conjunction with a liquid-nitrogen-cooled cryoshroud, achieved the required thermal conditions for the qualification tests. This report focuses on the design and analysis of the planar arrays based on first principles. Computational spreadsheets are included in the report.

Introduction

Since the B-2 chamber currently has no large-aperture collimated *solar simulator*, it was decided to utilize components of the existing B-2 infrared (IR) *thermal simulator* to produce the incident flux needed for the CREST thermal-vacuum test. A sufficient quantity of 12 ft infrared line sources and power control channels were available. These were recently refurbished to operational status, and appeared to be a good fit for this application considering the size of the test article and the quantity of units available. The line sources were assembled into planar arrays, each incident on the appropriate test article surface.

From the beginning it was readily apparent that the solar and infrared spectra had to be reconciled and the incident infrared flux density adjusted to transfer the correct *solar energy equivalent* to the test article.

Requirements

With the B-2 vacuum chamber operating at 3 torr, and the cryoshroud at 77.2 K, provide the following solar simulation:

1. The equivalent heating of one low Earth orbit (LEO) sun at 1 AU at 22° incident on the front (+*X*) and top (+*Y*) surfaces of the test article.
2. The equivalent heating of earth's albedo at levels of 0.65 and 0.95 LEO sun incident on the bottom (–*Y*) surface of the test article.
3. Manually controlled auxiliary heating at a level of 0.5 LEO sun incident toward the rear (–*X*) surface of the test article.
4. While the incident flux uniformity wasn't specified by the customer, a nominal tolerance band of ±5 percent was mutually agreed upon by the customer and NASA.

Engineering Approach

The Antarctic LEO sun was resolved into horizontal and vertical components of 0.927 and 0.375 sun, respectively, with separate planar lamp arrays provided for the front and top surfaces. The bottom surface (albedo) was heated by a third array, and a single line array was provided to supply auxiliary heat to the rear surface of the test article. A profile of the complete test setup is shown in Figure 1. The terms "surface," "face," and "zone" all refer to the heated outer surfaces of the test article and are used interchangeably throughout this report.

The infrared line sources were assembled into appropriately sized planar arrays. The line sources were spaced and aimed, and their individual power levels proportioned to optimize the transverse (perpendicular to line source axis) incident flux uniformity of each planar array. In Figure 1, the end view of each line source is shown. Figure 2 and Figure 3 show a portion of the arrays as installed in the vacuum chamber.

In the longitudinal (parallel to line source axis) direction, the line sources introduce the usual fall-off of flux density each side of center. The line sources also overhang the test article width somewhat, producing a small amount of heating on its normally dark side surfaces. Both of these undesirable characteristics are difficult to correct and were accepted by the customer as necessary tradeoffs.

The incident flux uniformity in the transverse direction was optimized based on theoretical prediction. Verification by optical scanning was considered, but was beyond the scope and budgetary constraints of this qualification test. According to the customer, it was sufficient that the *average* heating of each surface be equivalent to that produced by the 22° LEO sun.

Inside the vacuum chamber, the incident infrared flux levels were set to produce average surface heating equivalent to that of the 22° LEO sun, taking into account the optical properties of the surface films. The flux level settings were based on measurement of radiant energy absorbed by film test samples exposed first to the terrestrial sun and then to the infrared lamp arrays.

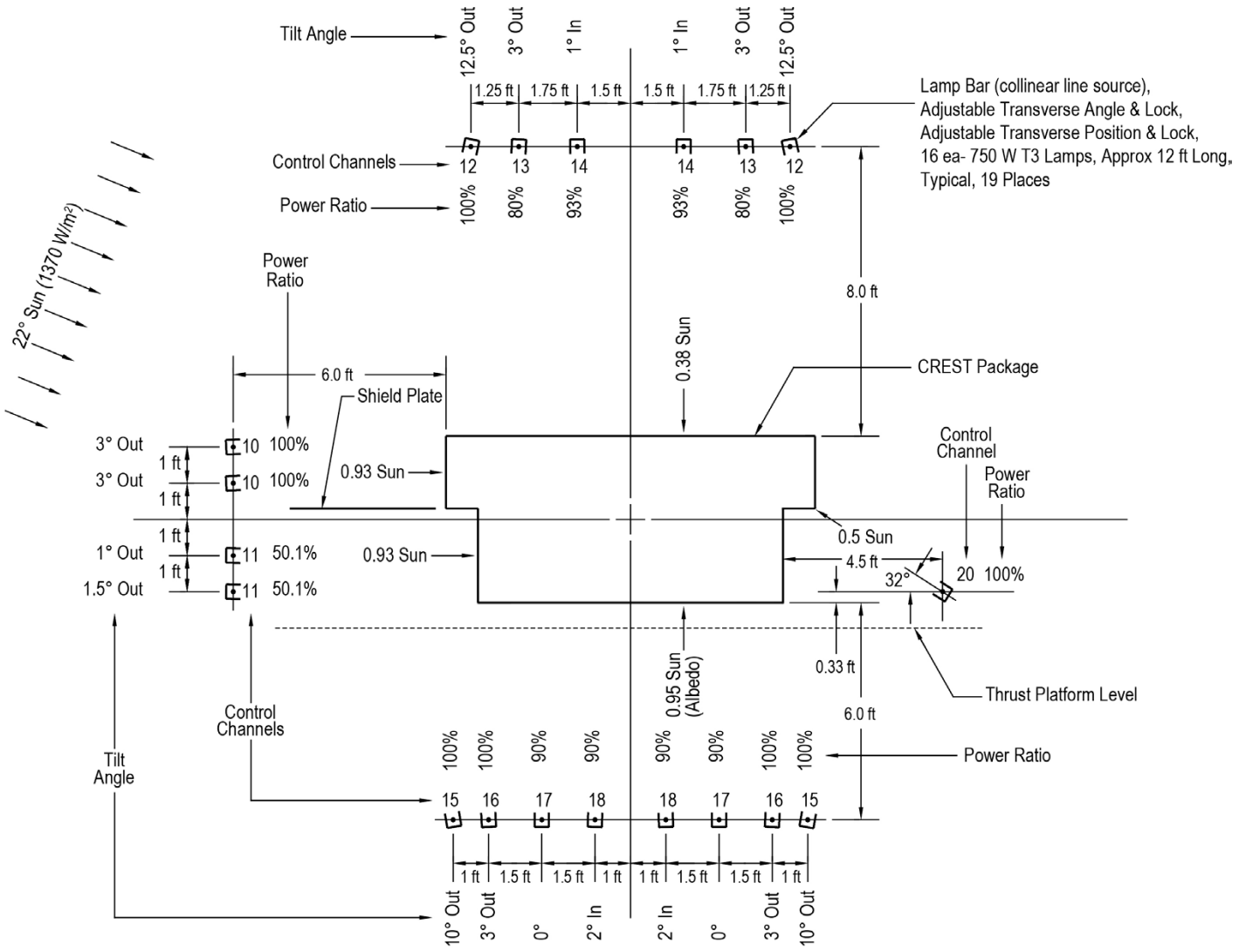

Figure 1.—Layout of infrared lamp arrays, CREST thermal-vacuum test.

Figure 2.—CREST package with top array and front array (far left).

Figure 3.—Top array lit during electrical checkout.

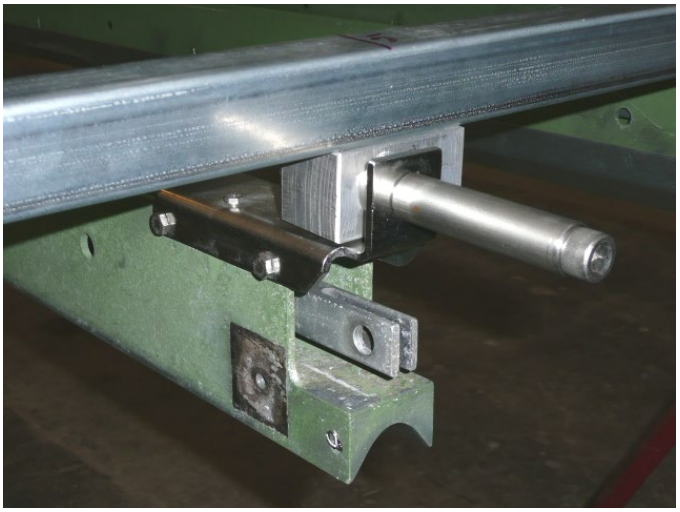

Figure 4.—Parabolic reflector and its adjustable mounting.

The Line Sources

Each 12 ft line source consists of 16 parallel-connected 120 V 750 W infrared quartz T3 lamps with the filaments collinearly oriented and closely spaced. The lamps share a common high-gain faceted aluminum parabolic reflector which projects a narrow wedge of illumination at high intensity. The reflector is cooled by radiation. See Figure 4.

When assembling a group of line sources into a planar array, the line sources must first be characterized. Following is a description of the three fundamental line source characteristics.

Projected Longitudinal Flux Distribution

The longitudinal projection characteristic of a single 12 ft line source is described by the following sequence of equations. This is a two-dimensional description where the line source and receiving line lie in the same plane. The 16 lamp filaments, each considered a unit point source, are oriented parallel to the receiving line. The flux density contribution (*ETU*) at the receiving line of each point source is given by:

$$A = -\tan^{-1}\frac{YS - YT}{XT - XS} \tag{1}$$

$$S = \sqrt{(YS - YT)^2 + (XT - XS)^2} \tag{2}$$

$$ETU = \frac{\cos^2 A}{S^2} \tag{3}$$

where

ETU	unit flux density contribution at receiving line
S	oblique distance from point source to receiving point
A	source angle and angle of incidence at receiving line (radians)
XS	horizontal source distance from origin to line array (ft)
YS	vertical distance from origin to point source (ft)
XT	horizontal distance from origin to receiving line
YT	vertical distance from origin to receiving point (ft)

For the longitudinal projection, each filament is treated as a point source if S is greater than or equal to ten times the filament length. Otherwise, the filaments should be divided into smaller elements and the elements treated as point sources. As shown in Figure 5, each sampled point on the receiving line represents a summation of the flux contributions from all 16 point sources. Figure 6 and Spreadsheet C.1 show the longitudinal flux distribution along the receiving line at a projection distance of 6 ft. The parabola-like flux density fall-off each side of center is an intrinsic projection characteristic of a line source.

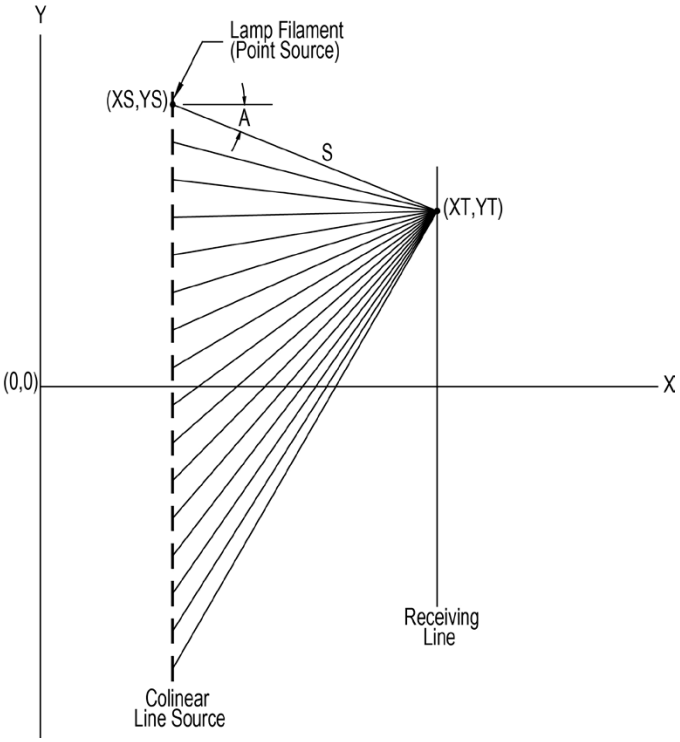

Figure 5.—Flux summation at receiving line.

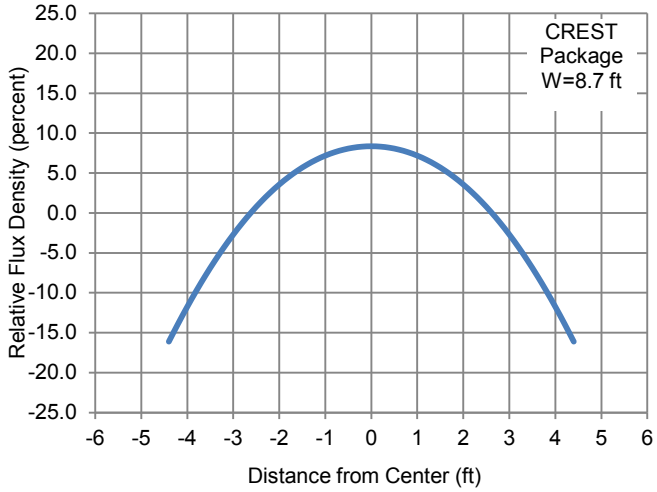

Figure 6.—Line source longitudinal flux distribution.

Projected Normal On-Axis Output Level

The flux producing capability of the line sources was determined by measurements made in the B-2 vacuum chamber during the course of the Integrated Systems Test (IST) conducted in April 2011. At full lamp voltage (120 V), three 12 ft line sources stacked vertically end-to-end produced approximately 1500 W/m^2 as read by a Hukseflux SR03-C01-05 thermopile pyranometer located at the midpoint, at a normal distance of 6 ft from the lamp filaments. Since the line sources were not stacked for the CREST test, the Hukseflux reading was converted to indicate what would have been generated by energizing the center 12 ft line source only.

By treating each lamp filament as a point source, the flux contributions of each filament were calculated using Equations (1), (2), and (3) and summed at the sensor location. This two-dimensional analysis was performed in Spreadsheet C.2 for both the 12 ft case and the 36 ft case. The flux density conversion was accomplished using the following proportionality.

$$EO_{12} = \frac{EO_{36} \cdot ET_{12}}{ET_{36}} \tag{4}$$

where

EO_{12} calculated normal on-axis flux density of a single 12 ft line source at 6 ft (W/m^2)

EO_{36} measured normal on-axis flux density of 36 ft line source at 6 ft (W/m^2)

ET_{12} average unit flux density at sensor from 12 ft unit line source (see Spreadsheet C.2)

ET_{36} average unit flux density at sensor from 36 ft unit line source (see Spreadsheet C.2)

Therefore,

$$EO_{12} = \frac{(1500\ \text{W/m}^2)\cdot(0.286)}{0.344} = 1247\ \text{W/m}^2$$

This result is a prediction of the full power radiant output of a single 12 ft line source that would have been read by the Hukseflux sensor at a normal distance of 6 ft from the source center.

Projected Radial Flux Distribution

The radial directional characteristic of a single line source is shown in Figure 7. This polar plot (Ref. 1) was produced by direct measurement of a 12 ft lamp/reflector assembly as part of the original acceptance testing of the B-2 thermal simulator components performed in 1965. Figure 8 shows the normalized directional characteristic in Cartesian form.

The following equation was developed to emulate the radial directional characteristic as a spreadsheet formula. It was fine-tuned by adjusting the exponents and angular coefficients to obtain a behavior that closely approximates the original directivity data.

$$D = \frac{16\cos^{16} A - 2.9\left(\dfrac{\cos(15A)}{(|57.3A|+1)^{0.2}}\right)}{13.1} \tag{5}$$

where

D normalized radial directivity function

A source angle or angular deviation from normal (radians)

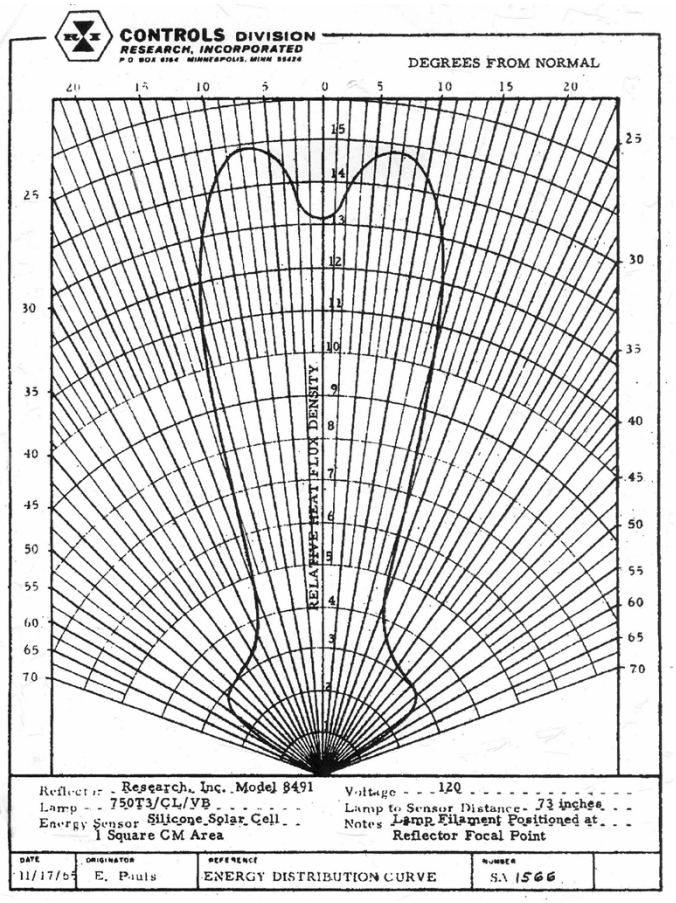

Figure 7.—Radial directional characteristic.

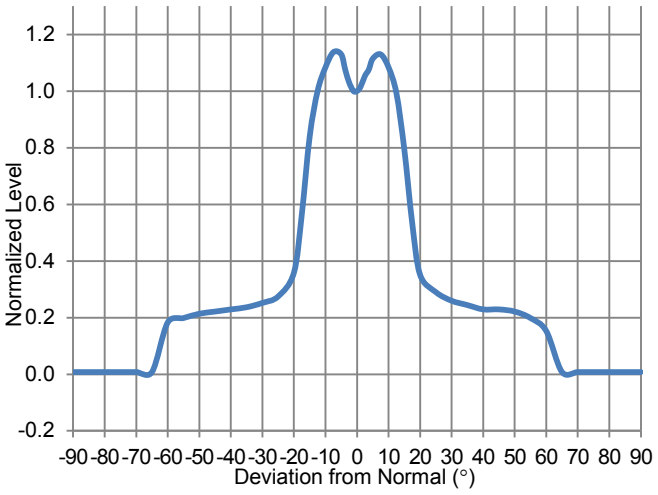

Figure 8.—Measured radial directivity.

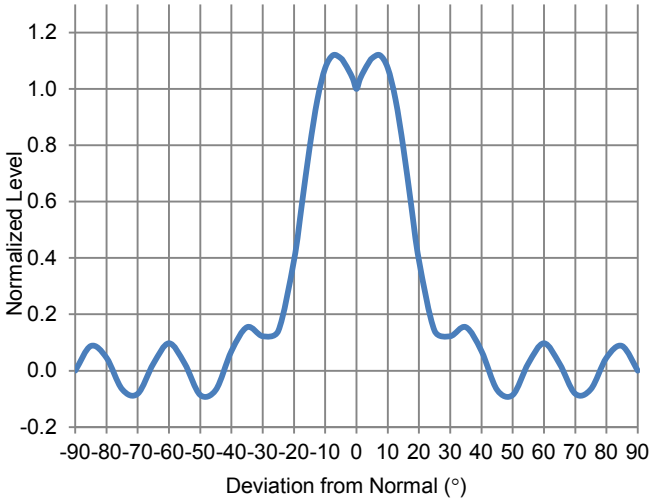

Figure 9.—Emulated radial directivity.

Direct radiation from the filaments at large angles (± 20° to ± 40°) was not included in the emulation. Figure 9 shows a directivity plot of Equation (5). Spreadsheet C.3 shows the original measured directivity data along with the emulated directivity data.

The following sequence of equations mathematically projects the flux density contribution of a single 12 ft line source onto the receiving plane. Here, the line source and receiving plane, or test article surface, are both perpendicular to and are bisected by the *XY* plane, and their intersections with the plane represent a point source and transverse receiving line respectively in the two-dimensional analysis. Figure 10 shows the geometric relationship of the projection. The projection is a locus of points (*ET* as a function of *YT*) along the receiving line describing the transverse flux density distribution. Note that once the projection occurs, the flux distribution terminology transitions from "radial" to "transverse". The flux density (*ET*) at each sampled point on the receiving line is given by:

$$A = -\tan^{-1}\frac{YS - YT}{XT - XS} \tag{1}$$

$$S = \sqrt{(YS - YT)^2 + (XT - XS)^2} \tag{2}$$

$$G = -B + A \tag{6}$$

$$D = \frac{16\cos^{16} G - 2.9\left(\dfrac{\cos(15G)}{(|57.3G| + 1)^{0.2}}\right)}{13.1} \tag{7}$$

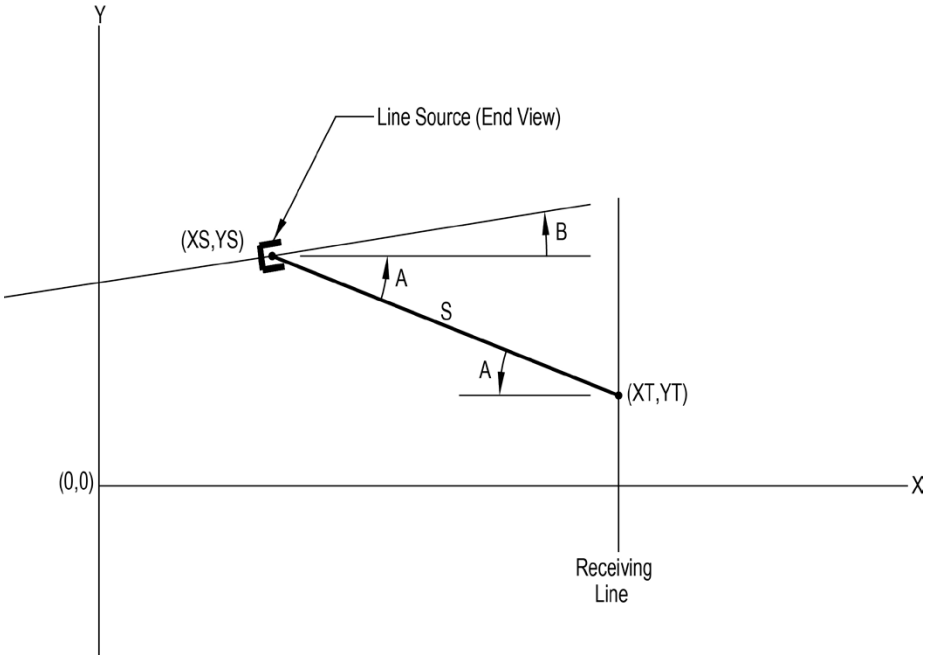

Figure 10.—Flux projection from a single source.

$$ET = 2.93(EO_{12})D(\cos A)\frac{R}{S^U} \qquad (8)$$

where

ET	flux density at receiving line (W/m^2)
A	source angle and angle of incidence at receiving line (radians)
S	oblique distance from point source to receiving line (ft)
G	substitution variable ($-B+A$)
D	normalized radial directivity function
B	reflector offset angle (radians)
R	original (IST) source-to-sensor distance (6 ft)
U	1.6 (see Appendix A)
EO_{12}	1247 W/m^2 (from Eq. (4))
XS	horizontal source distance from origin to line array (ft)
YS	vertical distance from origin to point source (ft)
XT	horizontal distance from origin to receiving line (ft)
YT	vertical distance from origin to receiving point (ft)

Figure 11 and Spreadsheet C.4 show the projected transverse flux distribution for a single line source. Note that Equation (8) is referenced to a 6 ft source-to-sensor distance, i.e., when S = 6 ft and A = 0 radians, the value of ET is EO_{12} (1247 W/m^2).

Sizing the Planar Arrays

The size of an array refers to its area as well as the quantity and wattage of the IR lamps employed. For the CREST test the lamps are arranged in collinear groups of 16, each forming a 12 ft line source, so the design challenge is to determine the

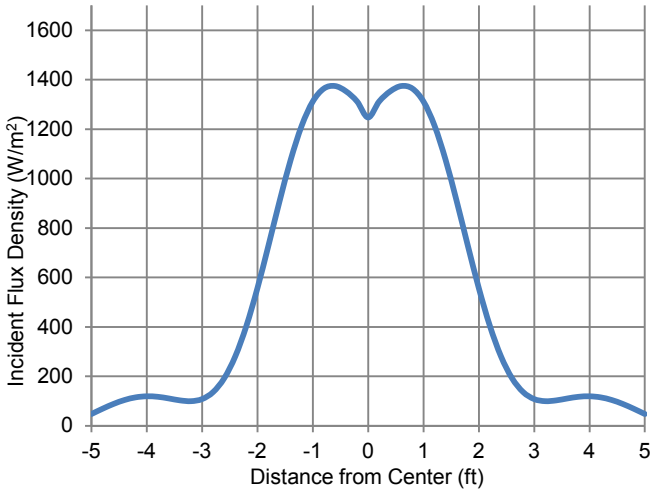

Figure 11.—Projected transverse flux distribution with line source at 6-ft distance.

number and spacing of the line sources for each heated face of the test article, such that each array will have sufficient heating capacity plus a generous (at least 50 percent) margin.

Initially we are merely estimating the number of line sources needed in the array based on the response of the Hukseflux pyranometer to the IR-rich lamp spectrum. In terms of infrared heating capability, this estimate will be conservative because the Hukseflux (wavelength range 0.305 to 2.8 μm) favors the solar spectrum, but is blind to much of the long wave radiation produced by the lamps (Ref. 2). Assuming an original in-chamber measurement of EO_{36} at 6 ft, the size of each lamp array can be estimated as follows:

$$N_E = SF \cdot \frac{ES}{EO_{12}} \cdot \frac{WT}{WS} \cdot \frac{S^{1.6}}{R \cdot (2.93)} \qquad (9)$$

where

N_E estimated number of line sources in planar array
SF required incident sun fraction
ES 1370 W/m^2 (one LEO sun)
EO_{12} 1247 W/m^2 (from Eq. (4))
WT transverse length of test article face (ft)
WS projected transverse beam width at ½ power points (ft)
S normal distance from filament plane to test article surface (ft)
R original (IST) source-to-sensor distance (6 ft)

Example:
For the CREST bottom zone:

$$N_E = 0.95 \cdot \frac{1370\ \text{W/m}^2}{1247\ \text{W/m}^2} \cdot \frac{10.4\,\text{ft}}{3.4\,\text{ft}} \cdot \frac{6^{1.6}\,\text{ft}}{(6\,\text{ft}) \cdot (2.93)} = 3.19$$

In order to reduce the tendency of developing a hot spot at the center of the zone, it is desirable not to have a line source at the transverse center of the array. It is also desirable to preserve symmetry about the transverse center when laying out the array. Therefore *N,* the number of line sources in the array, should be an even integer. The value *N* is then rounded up to the next higher even integral value, and the margin (*M*) and relative lamp power (*RLP*) values calculated over a range of increasing even values of *N*.

$$M = \left(\frac{N}{N_E} - 1 \right) \cdot 100 \qquad RLP = \frac{N_E}{N} \cdot 100$$

For N = 4: M = 25.4 percent RLP = 79.8 percent
For N = 6: M = 88.1 percent RLP = 53.2 percent
For N = 8: M = 151 percent RLP = 39.9 percent

From a flux density margin standpoint, the N = 6 case would probably be a good choice. In producing 0.95 IR suns, the lamps would run at only 53.2 percent of their full power capability, thus assuring long lamp life. However, for the CREST bottom zone it was decided to err toward the conservative and go with N = 8 for the following reasons:

a. Our design experience with these line sources was limited.
b. A higher value of N would enhance the transverse incident flux uniformity.
c. Tight scheduling required that the arrays be designed before the analysis tools were fully developed.

The sizing method just described provides the starting point for the layout and optimization processes. Compared to the final optimized array, it tends to overestimate the margin somewhat because it doesn't take into account the measures implemented to optimize the transverse flux uniformity.

Layout of the Planar Arrays

For the CREST configuration, array layout means transverse positioning and spacing of the line sources within the boundaries of the heated zone. The end line sources are positioned near the boundaries but must remain within the boundaries to prevent crosstalk to the adjacent zones. The remaining line source positions should initially be evenly spaced between the end ones, with all positions symmetrical about the center of the zone. When optimizing the flux uniformity it may be necessary to introduce a mild spacing gradient favoring the zone boundaries, while still maintaining symmetry about the center. The gradient will compensate for the natural flux density falloff as the boundaries are approached (Ref. 3).

Each power controller channel is capable of powering three line arrays. For the CREST test each channel powers a transverse symmetrical pair of line sources. In addition to providing a well-balanced array, the symmetry serves as a trouble-shooting aid if a layout or computational problem arises.

If possible, the final line source positions should be specified to fall on major division markings of the layout ruler to aid the technician in positioning the line sources. It's highly recommended to make all line source positions and aiming angle settings mechanically adjustable.

Optimizing Flux Uniformity

The sizing and layout methods just described will produce an array that is conservative in terms of flux density margin and lamp operating level. In general, flux uniformity and layout take precedence over sizing, and the array margin is increased as necessary to fulfill a desired layout sweet spot. As the number of line sources grows, the electrical power level can be reduced accordingly to maintain the correct average incident flux density level.

In the longitudinal direction, the flux uniformity for an array of line sources is described by Equations (1), (2), and (3), Figure 6, and Spreadsheet C.1. The parabola-like fall-off is intrinsic to the line source and little can be done to improve the longitudinal flux uniformity. This characteristic can be flattened somewhat by removing a few central lamps or by decreasing the distance from the array to the irradiated surface. However, for the CREST test, the customer agreed to live with the amount of fall-off shown in Figure 6, across the width of the test article, with the line source bars fully populated with lamps.

In the transverse direction, three line source adjustment parameters (degrees of freedom) exist and are defined as follows:

1. Line Source Position
   a. The transverse distance of a line source to the array centerline.
2. Offset Angle

a. The transverse angular deviation of line source reflector from normal incidence.

3. Power Ratio
   a. The power drive level of an individual line source within an array divided by the maximum line source drive level within the array. This ratio is expressed as a percentage. One 100 percent channel per array is considered the master to which all others are slaved by an assigned power ratio. Normally the line sources of like power ratio are paired symmetrically about the center.

The flux uniformity optimization process is a trial and error procedure whereby the designer manually adjusts the above parameters in a two-dimensional mathematical model of the array and observes the effect of each adjustment on the calculated transverse flux distribution. The optimizations are performed for each degree of freedom in the order shown above.

The mathematical model produces a summation of the flux contributions of all the line sources within the array at each selected sampling point on the receiving line. The model is based on Equations (1), (2), (6), (7), and (8), and is implemented in Spreadsheet C.4 through Spreadsheet C.13. For each line source, the designer inputs the parameters *XS*, *YS*, *XT*, *YT*, *B*, and *E*0 in the columns, and the output produced is a plot of relative flux density versus distance from the center of the receiving line. Also, the average flux density (*ET* average) at the longitudinal center of the zone is calculated and should be monitored as the optimization proceeds. If the average flux density is not satisfactory it might be necessary to adjust *N* (the number of line sources in the array) up or down to restore the desired margin. It also may be necessary to increase *N* in order to achieve satisfactory transverse flux uniformity.

The bottom (albedo) zone is used as a design example. Figure 12 and Spreadsheet C.5 show the flux uniformity obtained with the line source positions shown in Figure 1, with $B = 0$, and the power ratios at 100 percent. For CREST the line source positions were not optimized, but were based on a best guess because the analysis tools were not fully developed when the line source positions for all the zones were specified. This was done so that the mechanical build-up could proceed on schedule.

Figure 13 and Spreadsheet C.6 show the flux uniformity obtained with the tilt angles (*B*) optimized, and Figure 14 and Spreadsheet C.7 show the flux uniformity obtained with the power ratios also optimized. The final angles and power ratios for the bottom zone are shown in Figure 1. The improvement in uniformity obtained at each level of optimization is readily apparent. It was necessary to tilt the end line sources out almost beyond the zone boundaries in order to keep the flux density relatively flat out to the boundaries. Figure 15 and Spreadsheet C.8 show an overlay of the optimized contributions of each of the line sources.

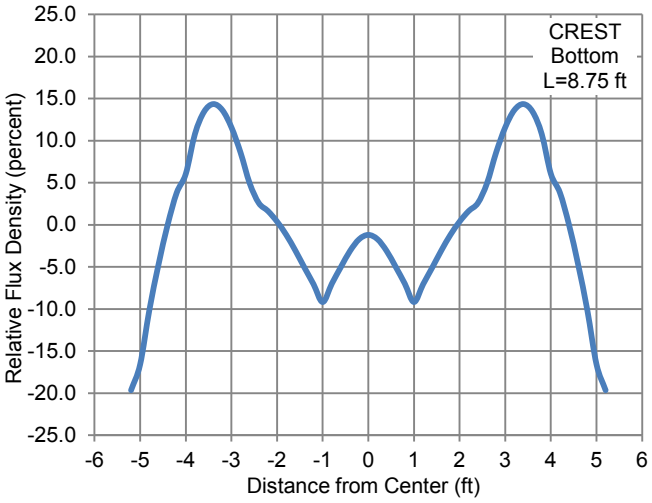

Figure 12.—Bottom zone not optimized.

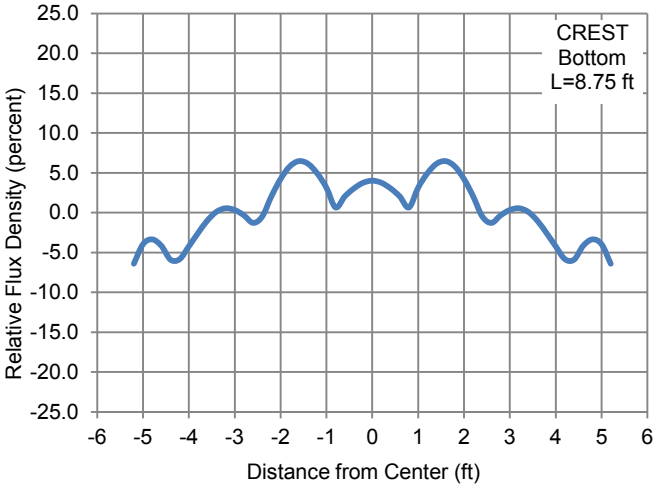

Figure 13.—Bottom zone tilt angles optimized.

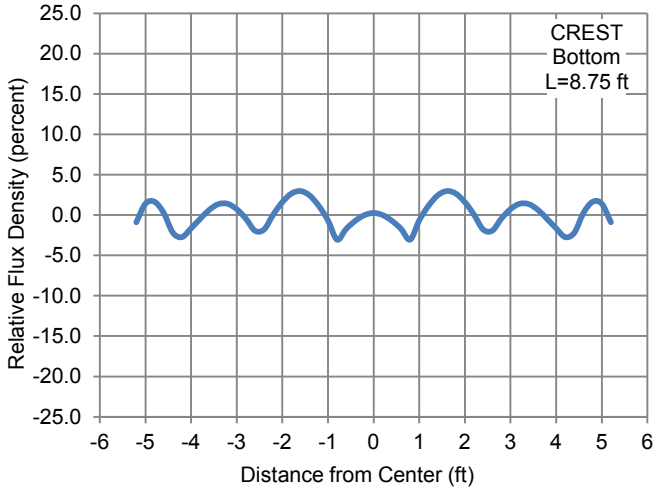

Figure 14.—Bottom zone tilt angles and power ratios optimized.

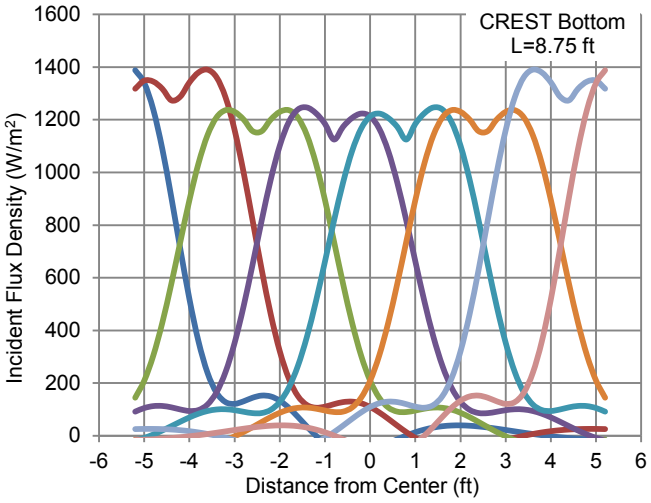

Figure 15.—Bottom zone line array contributions superimposed.

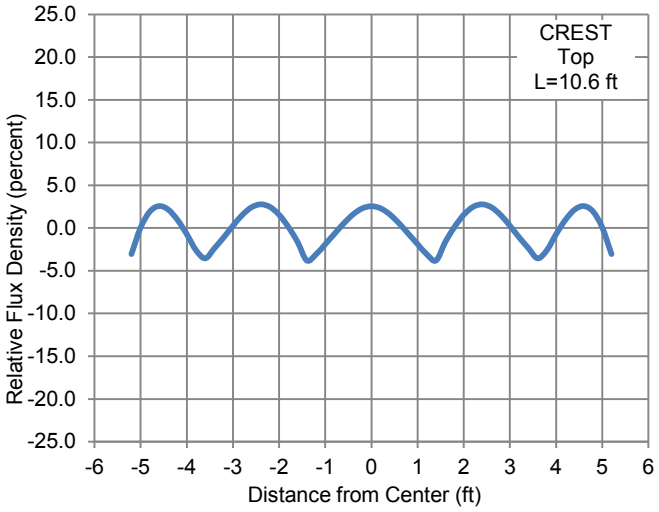

Figure 16.—Top zone tilt angles and power ratios optimized.

TABLE 1.—CREST PLANAR ARRAYS

Zone	Face dimensions, ft by ft	Required flux density, LEO suns	Full power flux density, IR suns	Full power flux density, W/m^2	Line sources, N	Total lamps, 750 W ea.	Max. power, kW	Distance to face [*XT-XS*], ft	Figure	Spreadsheet
Bottom	8.75 by 8.7	0.95	2.15	2943	8	128	96	6	Figure 14	Spreadsheet C.7
Top	10.6 by 8.7	0.375	1.2	1638	6	96	72	8	Figure 16	Spreadsheet C.9
Front Upper	2.08 by 8.7	0.927	2.04	2793	2	32	24	6	Figure 17	Spreadsheet C.10
Front Lower	2.69 by 8.7	0.927	1.64	2252	2	32	24	6.83	Figure 18	Spreadsheet C.11
Rear	----------	0.5	1.37	1880	1	16	12	4.27	Figure 22	Spreadsheet C.13

The Crest Planar Arrays

The solar simulation system built for the CREST thermal-vacuum test consisted of three planar arrays, each made up of several 12 kW infrared line sources. In each array, the 12 ft line sources spanned the 8.7 ft width of the test article with an overhang of approximately 1.6 ft on each side. Figure 1 shows the side view of the arrays, where the axes of the line sources are normal to the plane of the figure. The line sources for each zone were supported by a steel frames which surrounded the test article. The frames held the line sources in the positions and at the tilt angles specified in Figure 1. The transverse positions and angles were made adjustable by design.

Of the twelve 36 kW SCR power controllers available at the facility, ten were used to power the infrared lamps. Two 12 kW line sources were assigned to each power control channel, where each line source of the pair were placed symmetrically about the center of each zone. Each pair is identified by a like control channel number in Figure 1. The previously discussed power ratios, also symmetrical about each zone center, are shown in Figure 1. Table 1 summarizes the sizing parameters of each CREST array, and lists the spreadsheet and figure numbers associated with the flux uniformity optimizations for each zone.

The front face of the CREST package was split into two zones separated by a thin galvanized steel shield plate as shown in Figure 1. The front upper zone surface (detector housing), covered with aluminized Mylar film, projected out 11 in. from the lower surface (gondola) which was wrapped with a silver-Teflon film. Since the two films have different IR absorption characteristics, it was necessary to operate the upper and lower lamp banks at different power levels. The shield plate prevents radiant crosstalk between these zones.

The shield plate also acts as a partial reflector, producing an image of the two line sources of the zone. The reflectivity of the galvanized plate was assumed to be approximately 0.5, making the image contribution to the incident flux half that of the direct line sources. The images are entered into Spreadsheet C.10 and Spreadsheet C.11 as additional sources of reduced intensity at the image positions. Thus, the images are taken into account when optimizing the flux uniformity for these two zones. The theoretical flux uniformities achieved are shown in Figure 17 and Figure 18.

Figure 19 and Figure 20 show the transverse distribution of the flux incident on the bottom surface of the front and rear projections. These distributions are referenced to the average flux incident on the bottom face of the gondola. They take into

account the shadows introduced by the gondola front and rear lower edges, and the reflections introduced by the silver-Teflon film wrap on its front and rear faces. The simulation of shadows and reflections was accomplished by the use of correction coefficient columns in Spreadsheet C.12 to correct the incident flux density. For the shadows, a coefficient of 1.000 transitioning to 0.000 was used to go from full transmission to full extinction. For the reflections, a direct incidence coefficient of 1.000 transitioning to 1.900 (direct plus reflected) was used. The width of the transitions (approx. 0.67 in.) as projected onto the bottom surfaces are an approximate 3:1 reduction of the line source reflector width of approximately 2.0 in. The geometry describing the shadow and reflection boundaries is shown in Figure 21.

Figure 19 and Figure 20 show that the incident flux density at bottom surface of the projections is quite low (less than 60 percent of the flux density at the gondola bottom surface). This is mainly due to the shadows and the increased distance from the bottom lamps. Because of this, supplementary heating was provided at the rear of the package at the customer's request, to be used if needed to prevent this area of the package from becoming too cold. This heating capability, composed of a single line source, is identified as control channel 20 in Figure 1. Its incident flux density and directional characteristic are described in Figure 22 and Spreadsheet C.13.

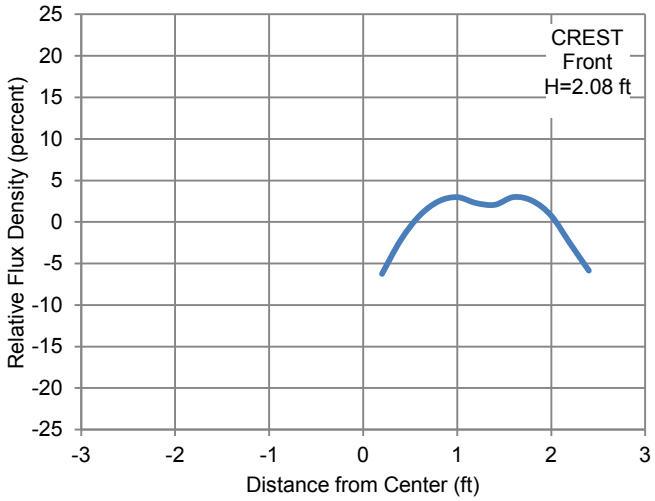

Figure 17.—Upper front zone optimized.

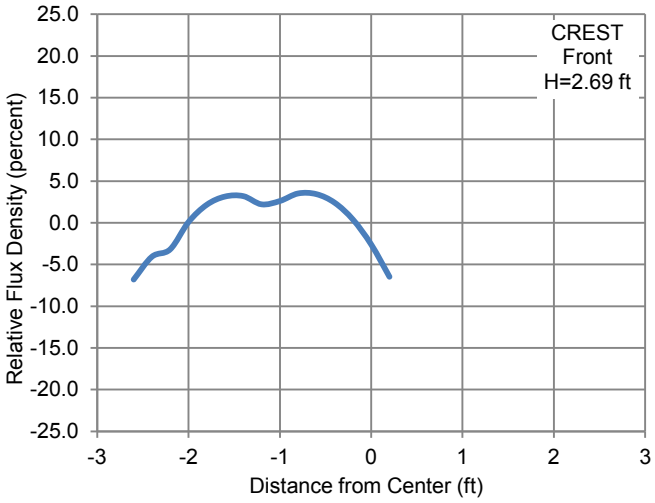

Figure 18.—Lower front zone optimized.

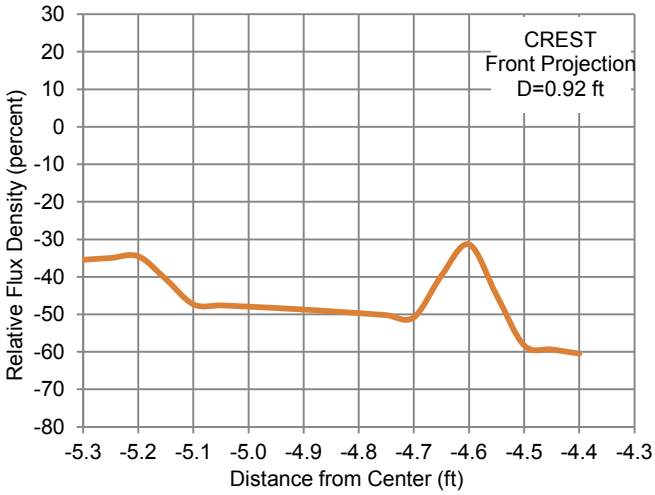

Figure 19.—Simulated albedo illumination of *front* projection bottom.

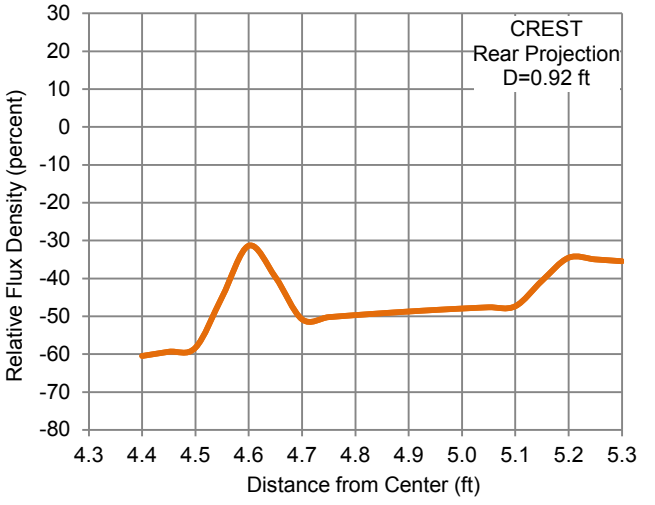

Figure 20.—Simulated albedo illumination of *rear* projection bottom.

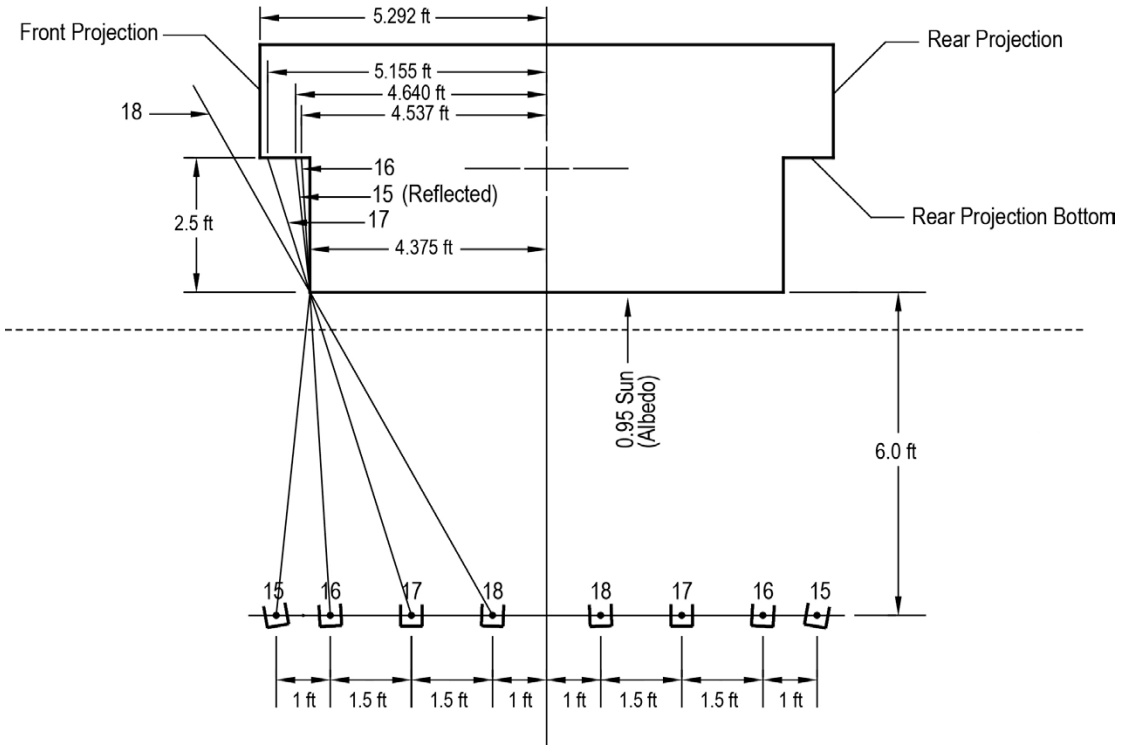

Figure 21.—Shadow and reflection boundaries affecting simulated albedo illumination of *front* projection bottom.

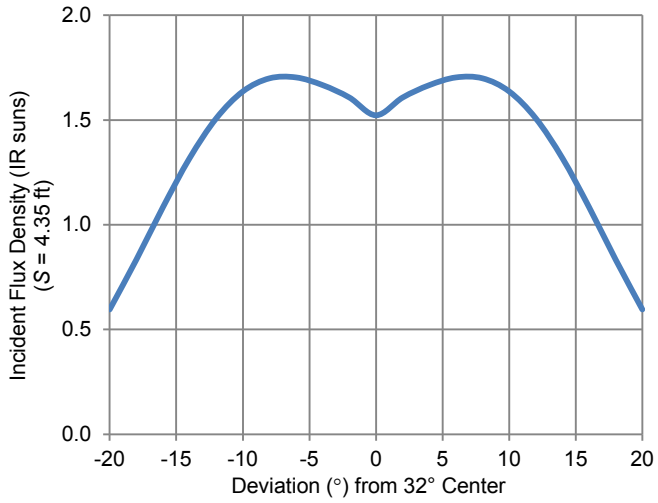

Figure 22.—Rear supplementary heat distribution.

Setting the Infrared Flux Density Levels

As mentioned previously, the CREST package was wrapped with two skin materials. The detector housing (the long upper portion) was wrapped with 4 mil aluminized Mylar film, while the gondola (shorter lower section) was wrapped with 5 mil silvered Teflon film. See Figure 1. The optical properties of these materials are wavelength sensitive and exhibit different absorption characteristics under T3 incandescent lamp illumination (2500 K) versus LEO solar illumination (6000 K). The optical properties of the skins under 2500 K illumination were not readily available from the manufacturers.

The objective is to simulate the LEO solar illumination using the T3 incandescent lamps in the vacuum chamber adjusted to transmit the equivalent heat flux is through the skins. The T3 illumination levels were developed using an empirical approach based on field measurements of terrestrial solar flux absorbed by skin samples. An instrument rake consisting of a 1 in. thick aluminum heat sink plate equipped with a Hukseflux SR03-C01-05 thermopile pyranometer and two Omega HFS-4 thin film thermopile heat flux sensors was constructed to enable the field measurements. See Figure 23. It is assumed that the spectral differences between the terrestrial sun and the LEO sun do not significantly affect the energy absorbed by the skins.

Terrestrial Sun Level

With the instrument rake set-up outdoors at high noon, the Hukseflux pyranometer was used to measure the density of the terrestrial sun flux incident on the rake. See Figure 23. The measurement was obtained by “shuttering” or intermittently casting a shadow on the pyranometer, where the terrestrial sun flux density was read as the difference between direct incident sun and shadow (diffuse skylight). A calibrated strip chart

recorder was used to record the pyranometer signal. See Figure 24 (lower trace). The *TSL* was calculated as follows:

$$TSL = \frac{A \cdot B}{C \cdot D} \tag{10}$$

where

TSL	terrestrial sun level (expressed in LEO suns)
A	pyranometer signal amplitude (expressed in chart *div*)
B	chart recorder calibration (*uV*/*div*)
C	pyranometer sensitivity (*uV*/W-m^2)
D	LEO solar constant (W/m^2)

Therefore,

$$TSL = \frac{(3.982 div)\cdot(2000 uV/div)}{(8.8 uV/\mathrm{W/m^2})\cdot(1370\ \mathrm{W/m^2\text{-}LEO\,sun})} = 0.661\,\mathrm{LEO\,sun}$$

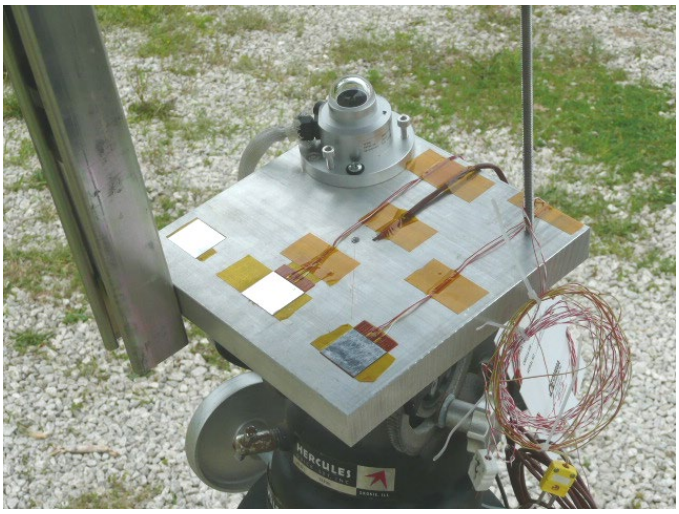

Figure 23.—Instrument rake set-up outdoors with Hukseflux Pyranometer (rear), and thin film heat flux sensors with material samples (front and left).

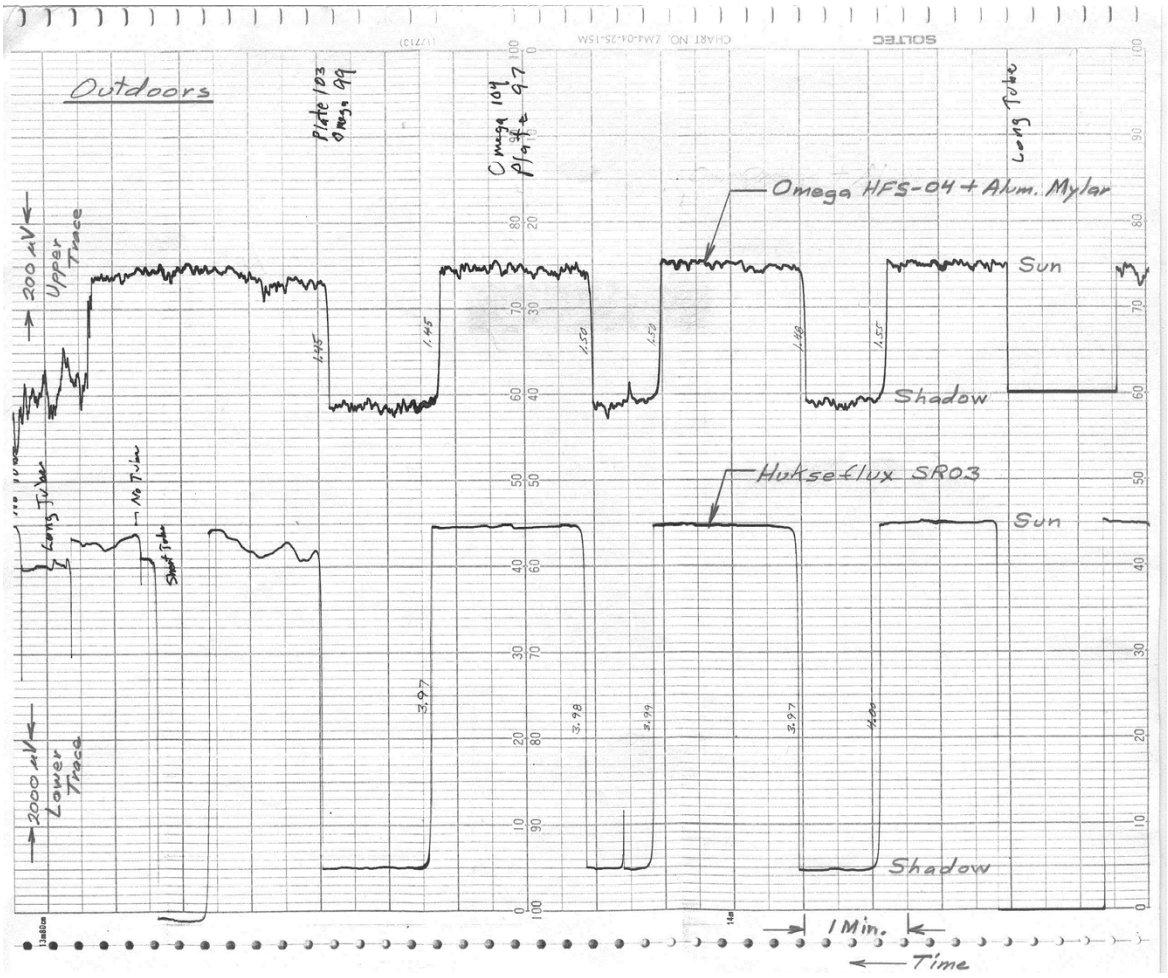

Figure 24.—Outdoor “shuttered” measurement of ISA for aluminized Mylar (upper trace) and accompanying pyranometer signal (lower trace).

Surface Film Evaluation

Aluminized Mylar Skin

The solar radiation absorption properties of the 4 mil aluminized Mylar film (second surface mirror side facing the Sun) were explored by attaching a sample to one of the Omega thin film thermopile heat flux sensors and exposing it to the terrestrial Sun. The back side of the sensor was adhered to the aluminum heat sink plate which was kept at ambient temperature prior to Sun exposure. A cardboard tube was installed to shield the sensor from outdoor wind disturbance. The sensor was shuttered from sun to shadow as previously described, and its output recorded on the strip chart. See Figure 24 (upper trace). The *ISA*, expressed in chart units (*div*), was read from the chart as step transitions between direct incident Sun and shadow. In generating the chart of Figure 24, the Omega sensor and the Hukseflux pyranometer were shuttered and recorded simultaneously to minimize differential errors caused by minor atmospheric and/or incident angle dynamics. The solar incident angle was manually kept very close to zero during the measurement period.

Using the *TSL* as the basis, the *ISA* was scaled down based on the required flux density to give the *SSA* as shown below.

$$SSA = \frac{ISA \cdot F}{TSL} \tag{11}$$

where

SSA scaled solar absorption (expressed in chart *div*)
ISA indicated solar absorption (expressed in chart *div*)
F required flux density (expressed in LEO suns)
TSL measured terrestrial sun level (expressed in LEO suns)

Therefore, for a required level of 0.375 LEO suns (top zone):

$$SSA = \frac{(1.488 div) \cdot (0.375 \text{ LEO suns})}{0.661 \text{ LEO sun}} = 0.844 div$$

The *ISA* and *SSA* values for all of the zones are given in Table 2 and Spreadsheet C.14.

Silvered Teflon Skin

The 5 mil silvered Teflon (second surface mirror side facing the sun) didn't absorb terrestrial solar energy well enough to permit a direct measurement of its ISA. Therefore, it was necessary to derive the ISA from the material's solar absorptance. The *typical* solar absorptance was estimated at 0.07 based on the manufacturers stated *maximum* value of 0.09. The *typical* solar absorptance was converted to the equivalent *ISA* as follows:

$$ISA = J \cdot TSL \cdot D \cdot \frac{K}{B} \tag{12}$$

where

ISA indicated solar absorption (expressed in chart *div*)
J solar absorptance for silvered Teflon (alpha)
TSL measured terrestrial sun level (expressed in LEO suns)
D LEO solar constant (W/m^2)
K heat flux sensor calibration (*uV*/W/m^2)
B chart recorder calibration (*uV*/*div*)

Therefore, for the bottom zone:

$$ISA = 0.07 \cdot (0.661 \text{ LEO sun}) \cdot (1370 \text{ W/m}^2 - \text{LEO sun}) \cdot \frac{2.2 uV/\text{W/m}^2}{200 uV/div} = 0.697 div$$

This result together with the required heating flux density (expressed in LEO suns) was substituted into Equation (11) above to give the *SSA* for the bottom zone at 0.95 LEO suns as follows:

$$SSA = \frac{ISA \cdot F}{TSL} \tag{11}$$

TABLE 2.—DEVELOPMENT OF CREST IN-CHAMBER ILLUMINATION LEVELS

Surface	Face dimensions, ft by ft	Required flux density, LEO suns	Skin material	Skin thickness, mils	ISA, div	SSA, div	SSA correction		CSSA, div
							Lg, %	Xv, %	
Bottom	8.75 by 8.7	0.95	Silvered Teflon	5	0.697	1.002	8.0	0.5	1.087
		0.65				0.685	8.0	0.5	0.744
Top	10.6 by 8.7	0.375	Aluminized Mylar	4	1.488	0.844	8.0	2.5	0.933
Front upper	2.08 by 8.7	0.927	Aluminized Mylar	4	1.488	2.087	8.0	2.0	2.295
Front lower	2.69 by 8.7	0.927	Silvered Teflon	5	0.697	0.977	8.0	2.5	1.080
Rear	----------	0.25	Aluminized Mylar	4	1.488	0.563	8.0	–3.0	0.591
		0.5				1.126	8.0	–3.0	1.182
		0.75				1.688	8.0	–3.0	1.773

$$SSA = \frac{(0.697 div) \cdot (0.95 \text{ LEO sun})}{0.661 \text{ LEO sun}} = 1.002 div$$

A later search of spacecraft thermal-control coating characteristics revealed that the correct solar absorptance for 5 mil silvered Teflon (Ref. 4) is 0.08. However, 0.07 was the value used in the calculations for the CREST test.

Corrections to SSA

Since, as previously shown, the flux distribution has residual transverse ripple and longitudinal parabola-like falloff, the *SSA* must be adjusted so that the average flux density produced for the zone is very close to the required level. Figure 16 shows the transverse ripple of the top zone. It can be seen that the flux density is approximately 2.5 percent high at the center (sensor location). Figure 6 shows the longitudinal distribution where the flux density is approximately 8 percent high at the center. Therefore, the SSA must be corrected as follows:

$$CSSA = SSA\left(1 + \frac{Lg + Xv}{100}\right) \tag{13}$$

where

CSSA corrected scaled solar absorption (expressed in chart *div*)
SSA scaled solar absorption (expressed in chart *div*)
Lg deviation due to longitudinal flux density fall-off (percent)
Xv deviation due to residual transverse ripple (percent)

Therefore, for the top zone:

$$CSSA = 0.844\left(1 + \frac{8.0 + 2.5}{100}\right) = 0.933 div$$

These corrections are summarized in Table 2 and Spreadsheet C.14 for all zones.

The instrument rake was then taken into the vacuum chamber, with the sensors placed at the center of the test article surface plane, and exposed to the quartz lamp arrays. See Figure 25. The voltage applied to the lamp array was adjusted to produce the *CSSA* calculated above as indicated by the chart recorder. At this level, the heating of the sample by the IR lamps is equivalent to the heating produced by 0.375 LEO suns. In effect, the IR heat lamps of the top zone are now "calibrated" at this sun level, skin material, voltage level, and sensor location.

Figure 26 (upper trace) shows a typical dynamic response to a voltage step applied to the lamps. It is believed that the initial rapid rise (right-hand side of chart) is caused by short-wave radiation directly from the lamp filaments, whereas the long exponential rise is due to radiation from the filaments being absorbed by the quartz envelopes and reradiated at longer wavelengths as the envelopes heat up less rapidly.

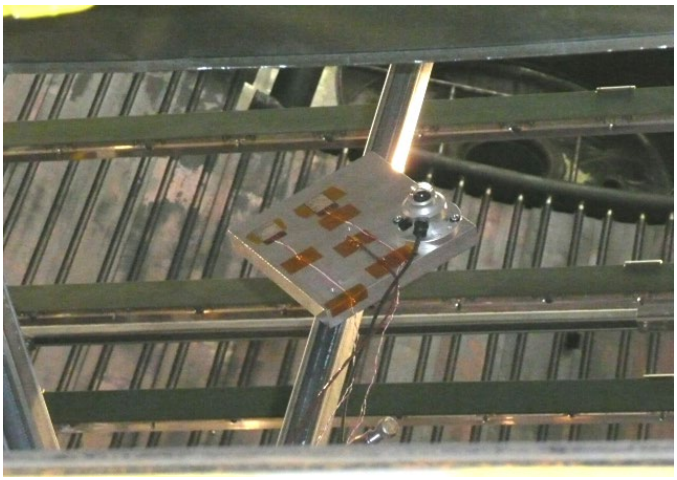

Figure 25.—Instrument rake setup in vacuum chamber.

Power Regulation Methodology

A Hukseflux pyranometer was installed at the center of each illuminated face of the test article for the purpose of providing a feedback signal to stabilize the incident flux density level. Even though the pyranometer doesn't cover the full infrared spectral range it was, in effect, "calibrated" when the lamp intensity levels were set in the chamber. These readings were subsequently used as setpoints for automatic closed-loop control of the incident flux levels. As a backup, the manual settings required to achieve the required flux levels in the chamber were also recorded, and could have been applied if manual control would have become necessary.

Small corrections were applied to the setpoint and manual values to compensate for chart reading errors which occurred in the test chamber environment when the intensity levels were set. These are calculated as follows.

Corrections to Automatic Control Setpoints

$$ACS = HF \cdot \frac{CSSA}{ICC} \tag{14}$$

where

ACS auto control setpoint (W/m^2)
HF Hukseflux pyranometer reading (W/m^2)
CSSA corrected scaled solar absorption (chart *div*)
ICC final in-chamber chart setting achieved (chart *div*)

Therefore, for the bottom zone:

$$ACS = \left(100 \text{ W/m}^2\right) \cdot \frac{1.09 div}{1.076 div} = 101.3 \text{ W/m}^2$$

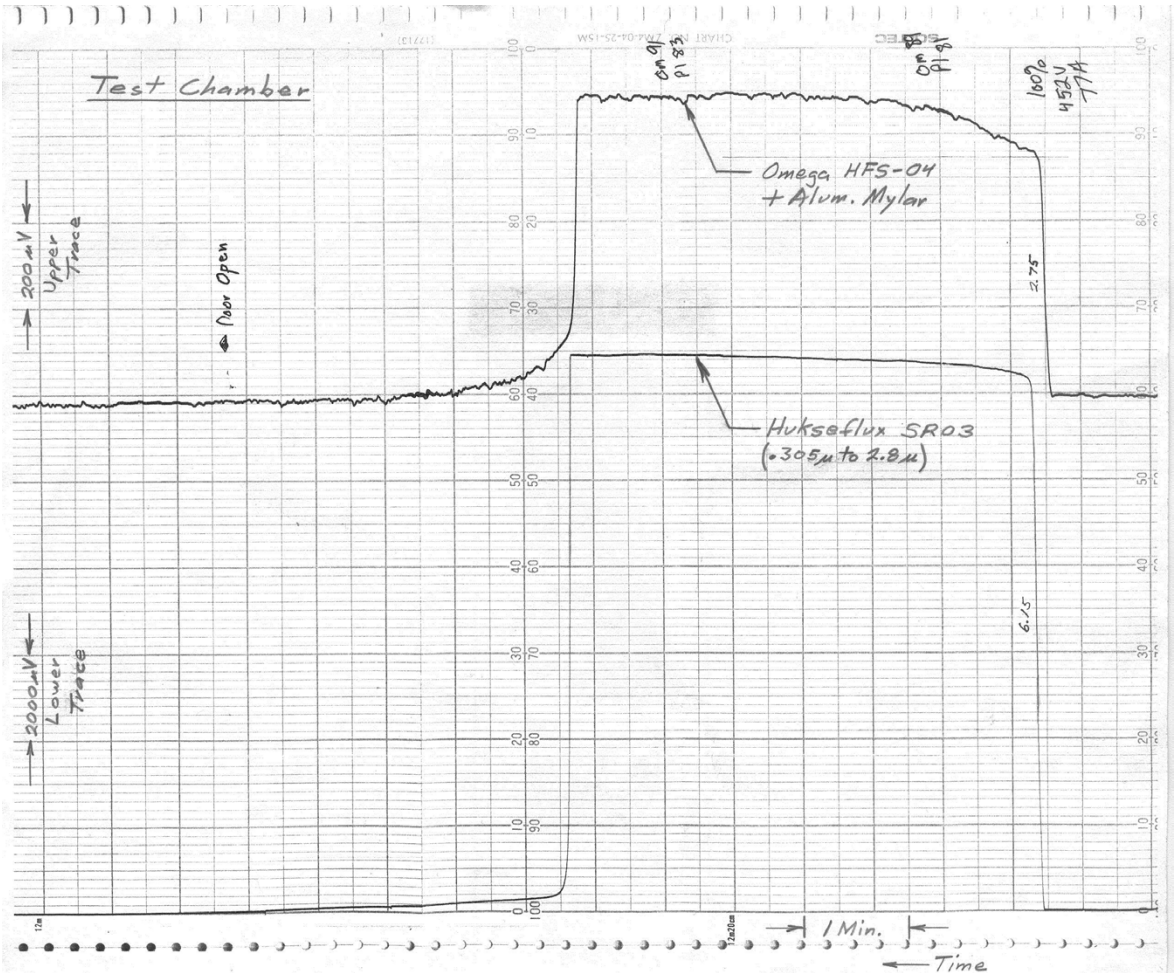

Figure 26.—In-chamber step response of lamp-sensor system. Aluminized Mylar on thin film thermopile (upper trace) Hukseflux pyranometer signal (lower trace)

Corrections to Manual Setpoints

$$CM = UM\left(\frac{CSSA}{ICC}\right)^{0.6} \tag{15}$$

where

CM corrected manual setting (percent)
UM uncorrected manual setting (percent)
CSSA corrected scaled solar absorption (chart *div*)
ICC final in-chamber chart setting achieved (chart *div*)

Therefore, for the bottom zone:

$$CM = (21.0 \text{ percent})\left(\frac{1.09div}{1.076div}\right)^{0.6} = 21.2 \text{ percent}$$

Note 1: For *CM*, 100 *percent* corresponds to the maximum voltage output (120 VAC) of the power control channel.
Note 2: The 0.6 exponent (Ref. 5) in Equation (15) accounts for the temperature-dependent filament resistance characteristic of incandescent lamps.

The above corrections as applied to the four control zones are calculated and summarized in Spreadsheet C.15 and Table 3 respectively. The *ACS* values were dialed-in to the thermal simulator programmable logic controller (PLC) as incident flux density setpoints based on what the Hukseflux sensors are seeing. When it was time to "turn on" the sun, these setpoints were enabled, and the infrared lamp arrays came up to the proper level to produce the required simulated solar heating of the test article surfaces. The manually controlled auxiliary heat provided at the rear of the package successfully maintained this region above the safe low temperature limit.

TABLE 3.—DEVELOPMENT OF CREST IN-CHAMBER POWER CONTROL LEVELS

Surface	Original illumination source	Required flux density, LEO suns	Skin material	Master channel	Hukseflux reading, W/m^2	Correction, CSSA/ICC	Auto control setpoint, W/m^2	Uncorrected manual, %	Correction, $CSSA/ICC^{0.6}$	Corrected manual, %
Bottom	Albedo	0.95 0.65	Silvered Teflon	15	100 52	1.013 1.000	101.3 52.0	21 17	1.008 1.000	21.2 17.0
Top	22° Sun	0.375	Aluminized Mylar	12	191	0.979	187.0	36	0.987	35.5
Front upper	22° Sun	0.927	Aluminized Mylar	10	700	0.962	673.2	50	0.977	48.8
Front lower	22° Sun	0.927	Silvered Teflon	[a]11	none	none	none	24.5	1.017	24.9
Rear	Dark Side	0.25 0.5 0.75	Aluminized Mylar	20	none	none	none	31 51 69	1.007 1.011 0.987	31.2 51.6 68.1

[a]Channel 11 command voltage slaved at 50.1 percent of channel 10.

Conclusion

This report described how we accomplished the solar simulation for CREST on a very tight time schedule, and to the extent possible, utilizing existing equipment. It heavily emphasized the development of planar arrays built from line sources, and the supporting theory. The customer was very pleased with the solar simulation achieved.

Appendix A.—Distance Exponent Development

When the receiving point is at a far distance from the line source, i.e., where the separation distance is more than ten times the length of the line source, the incident flux density at the receiving point varies approximately as the *inverse square* (Ref. 6) of the distance. When the receiving point is close to the line source, i.e., where the line source length is long compared to the separation distance, the incident flux density varies approximately as the *inverse* of the distance.

For the CREST test the transverse separation distances, (S) in Figure 10, ranged from 6 ft to approximately 13 ft. Compared to the 12 ft line sources, these separation distances fall into the intermediate range which suggests an inverse exponent which is greater than unity, but less than two.

This was explored mathematically by analyzing a single 12 ft line source where the receiving point was on a line perpendicular to and centered on the filament axis. The separation distance (*XT*-*XS*) was varied over the range of 6 to 13 ft as shown in Spreadsheet C.16. Several inverse exponential functions of distance were evaluated, plotted, and compared to the finite element analysis generated reference function (*ET* sum). Each was plotted as a function of the separation distance as shown in Figure 27. It can be seen that the inverse ($1/S$) and inverse squared $1/(S^2)$ functions diverged significantly from the reference, and the $1/(S^{SK})$ function tracked the best. Error-wise the $1/(S^{1.6})$ function is almost as good, and was ultimately chosen for CREST analysis work because of its simplicity.

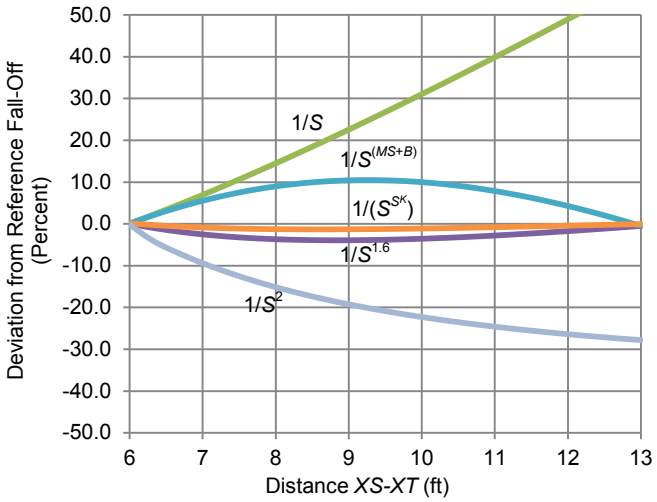

Figure 27.—Exponent development.

Appendix B.—B-2 Power Control Capability

The B-2 facility is equipped with twelve 60 Hz variable voltage power supply channels feeding the vacuum chamber for the purpose of operating incandescent lamps or heaters. These are transformer isolated feeds, each supplying 0 to 120 VAC 60 Hz single phase up to 50 KVA each. Each channel is SCR phase-angle controlled, and driven by command signals from a remotely located Programmable Logic Controller (PLC). The command signals can be controlled manually, or automatically utilizing feedback parameters and Proportional-Integral-Derivative (PID) algorithms. The PLC human operator interface is located in a separate control building approximately 2300 ft from the SCR power controllers.

Appendix C.—Spreadsheets

Spreadsheet C.1

Column A

↓

CREST001C

ARRAY BAR AXIAL DISTRIBUTION 05/27/2011

Lamp	XS(ft)	YS(ft)	XT	EO(W/m2)	YT	A(rad)	A(deg)	S(ft)	D	ET(W/m2)	ET Sum:
1.000	0.000	-5.625	6.000	1.000	4.400	1.031	59.099	11.683	0.514	0.002	0.221
2.000	0.000	-4.875	6.000	1.000	4.400	0.997	57.101	11.047	0.543	0.002	
3.000	0.000	-4.125	6.000	1.000	4.400	0.958	54.862	10.425	0.576	0.003	
4.000	0.000	-3.375	6.000	1.000	4.400	0.914	52.342	9.821	0.611	0.004	
5.000	0.000	-2.625	6.000	1.000	4.400	0.864	49.499	9.239	0.649	0.005	
6.000	0.000	-1.875	6.000	1.000	4.400	0.808	46.283	8.682	0.691	0.006	
7.000	0.000	-1.125	6.000	1.000	4.400	0.744	42.640	8.156	0.736	0.008	
8.000	0.000	-0.375	6.000	1.000	4.400	0.672	38.514	7.668	0.782	0.010	
9.000	0.000	0.375	6.000	1.000	4.400	0.591	33.855	7.225	0.830	0.013	
10.000	0.000	1.125	6.000	1.000	4.400	0.500	28.627	6.836	0.878	0.016	
11.000	0.000	1.875	6.000	1.000	4.400	0.398	22.823	6.510	0.922	0.020	
12.000	0.000	2.625	6.000	1.000	4.400	0.288	16.480	6.257	0.959	0.023	
13.000	0.000	3.375	6.000	1.000	4.400	0.169	9.694	6.087	0.986	0.026	
14.000	0.000	4.125	6.000	1.000	4.400	0.046	2.624	6.006	0.999	0.028	
15.000	0.000	4.875	6.000	1.000	4.400	-0.079	-4.526	6.019	0.997	0.027	
16.000	0.000	5.625	6.000	1.000	4.400	-0.201	-11.539	6.124	0.980	0.026	

YT Values	ET Sum	ET Average	Pct. Dev.
-4.400	0.221	0.264	-16.1
-4.200	0.227	0.264	-13.9
-4.000	0.233	0.264	-11.8
-3.800	0.238	0.264	-9.7
-3.600	0.243	0.264	-7.8
-3.400	0.248	0.264	-6.0
-3.200	0.252	0.264	-4.3
-3.000	0.257	0.264	-2.7
-2.800	0.261	0.264	-1.2
-2.600	0.264	0.264	0.1
-2.400	0.267	0.264	1.4
-2.200	0.270	0.264	2.5
-2.000	0.273	0.264	3.6
-1.800	0.276	0.264	4.5
-1.600	0.278	0.264	5.3
-1.400	0.280	0.264	6.0
-1.200	0.281	0.264	6.7
-1.000	0.283	0.264	7.2
-0.800	0.284	0.264	7.6
-0.600	0.285	0.264	7.9
-0.400	0.285	0.264	8.2
-0.200	0.286	0.264	8.3
0.000	0.286	0.264	8.4
0.200	0.286	0.264	8.3
0.400	0.285	0.264	8.2
0.600	0.285	0.264	7.9
0.800	0.284	0.264	7.6
1.000	0.283	0.264	7.2
1.200	0.281	0.264	6.7
1.400	0.280	0.264	6.0
1.600	0.278	0.264	5.3
1.800	0.276	0.264	4.5
2.000	0.273	0.264	3.6
2.200	0.270	0.264	2.5
2.400	0.267	0.264	1.4
2.600	0.264	0.264	0.1
2.800	0.261	0.264	-1.2
3.000	0.257	0.264	-2.7
3.200	0.252	0.264	-4.3
3.400	0.248	0.264	-6.0
3.600	0.243	0.264	-7.8
3.800	0.238	0.264	-9.7
4.000	0.233	0.264	-11.8
4.200	0.227	0.264	-13.9
4.400	0.221	0.264	-16.1

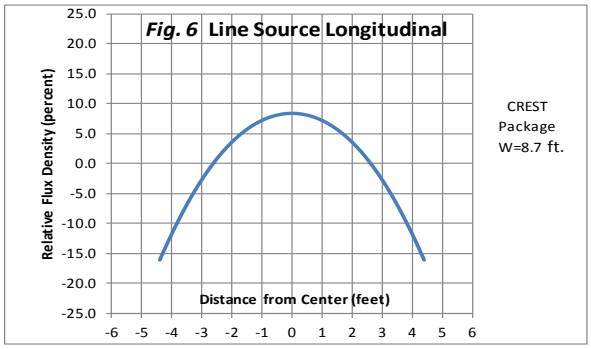

Formulas:
D = AVERAGE(C24:C68)
E = (C-D)/D*100

I = -ATAN((C-G)/(D-B))
J = H*180/3.1416
K = ((C-G)^2+(D-B)^2)^0.5

N = COS(I)
O = F*N*COS(I)/K^2
P = SUM(O4:O19)

Macro:
Sub CERST001CM()
Dim i As Long

For i = 24 To 68
Cells(4, 7) = Cells(i, 2)
Calculate
Cells(i, 3) = Cells(4, 16)
Next i
End Sub

Spreadsheet C.2

Column A
↓

CREST001B

ARRAY BAR RATIO CALIBRATION 05/27/2011 06/14/2011

Lamp	XS(ft)	YS(ft)	XT	EO(W/m2)	YT	A(rad)	A(deg)	S(ft)	D	ET(W/m2)	ET36 SUM(O4:O51)	
1.000	0.000	0.375	6.000	1.000	18.000	1.243	71.200	18.618	0.322	0.000	0.344	
2.000	0.000	1.125	6.000	1.000	18.000	1.229	70.427	17.910	0.335	0.000	"	
3.000	0.000	1.875	6.000	1.000	18.000	1.215	69.590	17.205	0.349	0.000	"	
4.000	0.000	2.625	6.000	1.000	18.000	1.199	68.682	16.504	0.364	0.000	"	
5.000	0.000	3.375	6.000	1.000	18.000	1.181	67.694	15.808	0.380	0.001	"	
6.000	0.000	4.125	6.000	1.000	18.000	1.163	66.615	15.117	0.397	0.001	"	
7.000	0.000	4.875	6.000	1.000	18.000	1.142	65.433	14.431	0.416	0.001	"	
8.000	0.000	5.625	6.000	1.000	18.000	1.119	64.133	13.753	0.436	0.001	"	
9.000	0.000	6.375	6.000	1.000	18.000	1.094	62.700	13.082	0.459	0.001	"	
10.000	0.000	7.125	6.000	1.000	18.000	1.067	61.113	12.420	0.483	0.002	"	
11.000	0.000	7.875	6.000	1.000	18.000	1.036	59.349	11.769	0.510	0.002	"	
12.000	0.000	8.625	6.000	1.000	18.000	1.001	57.381	11.131	0.539	0.002	"	
13.000	0.000	9.375	6.000	1.000	18.000	0.963	55.175	10.507	0.571	0.003	"	
14.000	0.000	10.125	6.000	1.000	18.000	0.920	52.696	9.900	0.606	0.004	"	
15.000	0.000	10.875	6.000	1.000	18.000	0.871	49.899	9.315	0.644	0.005	"	ET12
16.000	0.000	11.625	6.000	1.000	18.000	0.816	46.736	8.754	0.685	0.006	"	SUM(O20:O35)
17.000	0.000	12.375	6.000	1.000	18.000	0.753	43.152	8.224	0.730	0.008	"	0.286
18.000	0.000	13.125	6.000	1.000	18.000	0.682	39.094	7.731	0.776	0.010	"	"
19.000	0.000	13.875	6.000	1.000	18.000	0.602	34.508	7.281	0.824	0.013	"	"
20.000	0.000	14.625	6.000	1.000	18.000	0.512	29.358	6.884	0.872	0.016	"	"
21.000	0.000	15.375	6.000	1.000	18.000	0.412	23.629	6.549	0.916	0.020	"	"
22.000	0.000	16.125	6.000	1.000	18.000	0.303	17.354	6.286	0.954	0.023	"	"
23.000	0.000	16.875	6.000	1.000	18.000	0.185	10.620	6.105	0.983	0.026	"	"
24.000	0.000	17.625	6.000	1.000	18.000	0.062	3.576	6.012	0.998	0.028	"	"
25.000	0.000	18.375	6.000	1.000	18.000	-0.062	-3.576	6.012	0.998	0.028	"	"
26.000	0.000	19.125	6.000	1.000	18.000	-0.185	-10.620	6.105	0.983	0.026	"	"
27.000	0.000	19.875	6.000	1.000	18.000	-0.303	-17.354	6.286	0.954	0.023	"	"
28.000	0.000	20.625	6.000	1.000	18.000	-0.412	-23.629	6.549	0.916	0.020	"	"
29.000	0.000	21.375	6.000	1.000	18.000	-0.512	-29.358	6.884	0.872	0.016	"	"
30.000	0.000	22.125	6.000	1.000	18.000	-0.602	-34.508	7.281	0.824	0.013	"	"
31.000	0.000	22.875	6.000	1.000	18.000	-0.682	-39.094	7.731	0.776	0.010	"	"
32.000	0.000	23.625	6.000	1.000	18.000	-0.753	-43.152	8.224	0.730	0.008	"	"
33.000	0.000	24.375	6.000	1.000	18.000	-0.816	-46.736	8.754	0.685	0.006	"	
34.000	0.000	25.125	6.000	1.000	18.000	-0.871	-49.899	9.315	0.644	0.005	"	
35.000	0.000	25.875	6.000	1.000	18.000	-0.920	-52.696	9.900	0.606	0.004	"	
36.000	0.000	26.625	6.000	1.000	18.000	-0.963	-55.175	10.507	0.571	0.003	"	
37.000	0.000	27.375	6.000	1.000	18.000	-1.001	-57.381	11.131	0.539	0.002	"	
38.000	0.000	28.125	6.000	1.000	18.000	-1.036	-59.349	11.769	0.510	0.002	"	
39.000	0.000	28.875	6.000	1.000	18.000	-1.067	-61.113	12.420	0.483	0.002	"	
40.000	0.000	29.625	6.000	1.000	18.000	-1.094	-62.700	13.082	0.459	0.001	"	
41.000	0.000	30.375	6.000	1.000	18.000	-1.119	-64.133	13.753	0.436	0.001	"	
42.000	0.000	31.125	6.000	1.000	18.000	-1.142	-65.433	14.431	0.416	0.001	"	
43.000	0.000	31.875	6.000	1.000	18.000	-1.163	-66.615	15.117	0.397	0.001	"	
44.000	0.000	32.625	6.000	1.000	18.000	-1.181	-67.694	15.808	0.380	0.001	"	
45.000	0.000	33.375	6.000	1.000	18.000	-1.199	-68.682	16.504	0.364	0.000	"	
46.000	0.000	34.125	6.000	1.000	18.000	-1.215	-69.590	17.205	0.349	0.000	"	
47.000	0.000	34.875	6.000	1.000	18.000	-1.229	-70.427	17.910	0.335	0.000	"	
48.000	0.000	35.625	6.000	1.000	18.000	-1.243	-71.200	18.618	0.322	0.000	"	

Formulas:
I = -ATAN((C-G)/(D-B))
J = I*180/3.1416
K = ((C-G)^2+(D-B)^2)^0.5

N = COS(I)
O = F*N*COS(I)/K^2
P = SUM(O4:O51)
Q = SUM(O20:O35)

Spreadsheet C.3

Column A

↓

CREST001J

LINE ARRAY POLAR PLOT 07/20/2011

Bar	R(ft)	A(deg)	A(rad)	D
1.000	6.000	90.000	1.571	0.000

Column Heading Notes

RI Level: Reseasch Inc. Raw Directivity Data

RI Level/1.3: Normalized Measured Directivity, Fig 8

D Level: Emulated Directivity, Fig 9

A(deg)	RI Level	RI Level/1.31	D Level	Pct. Dev.
-90.000	0.010	0.008	0.000	-0.8
-85.000	0.010	0.008	0.088	8.0
-80.000	0.010	0.008	0.046	3.8
-75.000	0.010	0.008	-0.066	-7.3
-70.000	0.010	0.008	-0.082	-8.9
-65.000	0.010	0.008	0.025	1.7
-60.000	0.240	0.183	0.097	-8.6
-55.000	0.260	0.198	0.026	-17.3
-50.000	0.280	0.214	-0.086	-30.0
-45.000	0.290	0.221	-0.068	-28.9
-40.000	0.300	0.229	0.070	-15.9
-35.000	0.310	0.237	0.155	-8.2
-30.000	0.330	0.252	0.122	-13.0
-25.000	0.360	0.275	0.142	-13.3
-20.000	0.470	0.359	0.391	3.2
-17.500	0.740	0.565	0.588	2.3
-15.000	1.100	0.840	0.791	-4.8
-12.500	1.310	1.000	0.962	-3.8
-10.000	1.420	1.084	1.075	-0.9
-7.500	1.490	1.137	1.120	-1.8
-5.000	1.480	1.130	1.109	-2.1
-3.750	1.410	1.076	1.090	1.4
-2.500	1.350	1.031	1.066	3.6
-1.125	1.310	1.000	1.035	3.5
0.000	1.310	1.000	1.000	0.0
1.125	1.330	1.015	1.035	2.0
2.500	1.380	1.053	1.066	1.3
3.750	1.410	1.076	1.090	1.4
5.000	1.460	1.115	1.109	-0.5
7.500	1.480	1.130	1.120	-1.0
10.000	1.420	1.084	1.075	-0.9
12.500	1.300	0.992	0.962	-3.0
15.000	1.040	0.794	0.791	-0.3
17.500	0.700	0.534	0.588	5.4
20.000	0.460	0.351	0.391	4.0
25.000	0.380	0.290	0.142	-14.8
30.000	0.340	0.260	0.122	-13.7
35.000	0.320	0.244	0.155	-9.0
40.000	0.300	0.229	0.070	-15.9
45.000	0.300	0.229	-0.068	-29.7
50.000	0.290	0.221	-0.086	-30.8
55.000	0.260	0.198	0.026	-17.3
60.000	0.200	0.153	0.097	-5.5
65.000	0.010	0.008	0.025	1.7
70.000	0.010	0.008	-0.082	-8.9
75.000	0.010	0.008	-0.066	-7.3
80.000	0.010	0.008	0.046	3.8
85.000	0.010	0.008	0.088	8.0
90.000	0.010	0.008	0.000	-0.8

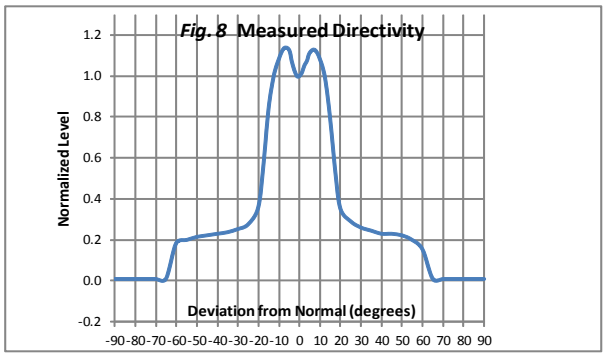

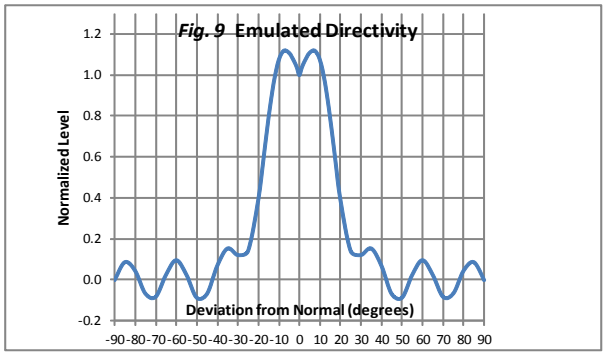

Formulas:

E4 = C4*3.1416/180

F4 = (16*(COS(E4))^16-2.9*COS(15*E4)/((((E4*57.3)^2)^0.5+1)^(1/5)))/13.1

D = C/1.31

F = (E-D)*100

Macro:

```
Sub CERST001JM()
Dim i As Long

For i = 12 To 60
Cells(4, 3) = Cells(i, 2)
Calculate
Cells(i, 5) = Cells(4, 6)
Next i
End Sub
```

Spreadsheet C.4

Column A

↓

CREST001A3A

REAR PROJECTION BOTTOM 05/27/2011 06/14/2011

Bar	XS(ft)	YS(ft)	XT	B(deg)	EO(W/m2)	YT	A(rad)	A(deg)	S(ft)	G(rad)	G(deg)	D	ET(W/m2)
1.000	0.000	0.000	6.000	0.000	1247.0	5.000	0.695	39.805	7.810	0.695	39.805	0.075	47.28

ET Sum: 47.28

YT Values	ET Sum	ET Average	IR Suns	Avg. IR Suns
-5.000	47.28	545.65	0.035	0.398
-4.800	68.62	545.65	0.050	0.398
-4.600	88.22	545.65	0.064	0.398
-4.400	104.19	545.65	0.076	0.398
-4.200	114.83	545.65	0.084	0.398
-4.000	119.10	545.65	0.087	0.398
-3.800	117.06	545.65	0.085	0.398
-3.600	110.36	545.65	0.081	0.398
-3.400	102.59	545.65	0.075	0.398
-3.200	99.34	545.65	0.073	0.398
-3.000	107.88	545.65	0.079	0.398
-2.800	136.31	545.65	0.099	0.398
-2.600	192.19	545.65	0.140	0.398
-2.400	280.87	545.65	0.205	0.398
-2.200	403.67	545.65	0.295	0.398
-2.000	556.56	545.65	0.406	0.398
-1.800	729.72	545.65	0.533	0.398
-1.600	908.40	545.65	0.663	0.398
-1.400	1075.25	545.65	0.785	0.398
-1.200	1213.69	545.65	0.886	0.398
-1.000	1311.54	545.65	0.957	0.398
-0.800	1363.91	545.65	0.996	0.398
-0.600	1374.27	545.65	1.003	0.398
-0.400	1352.90	545.65	0.988	0.398
-0.200	1311.93	545.65	0.958	0.398
0.000	1246.93	545.65	0.910	0.398
0.200	1311.93	545.65	0.958	0.398
0.400	1352.90	545.65	0.988	0.398
0.600	1374.27	545.65	1.003	0.398
0.800	1363.91	545.65	0.996	0.398
1.000	1311.54	545.65	0.957	0.398
1.200	1213.69	545.65	0.886	0.398
1.400	1075.25	545.65	0.785	0.398
1.600	908.40	545.65	0.663	0.398
1.800	729.72	545.65	0.533	0.398
2.000	556.56	545.65	0.406	0.398
2.200	403.67	545.65	0.295	0.398
2.400	280.87	545.65	0.205	0.398
2.600	192.19	545.65	0.140	0.398
2.800	136.31	545.65	0.099	0.398
3.000	107.88	545.65	0.079	0.398
3.200	99.34	545.65	0.073	0.398
3.400	102.59	545.65	0.075	0.398
3.600	110.36	545.65	0.081	0.398
3.800	117.06	545.65	0.085	0.398
4.000	119.10	545.65	0.087	0.398
4.200	114.83	545.65	0.084	0.398
4.400	104.19	545.65	0.076	0.398
4.600	88.22	545.65	0.064	0.398
4.800	68.62	545.65	0.050	0.398
5.000	47.28	545.65	0.035	0.398

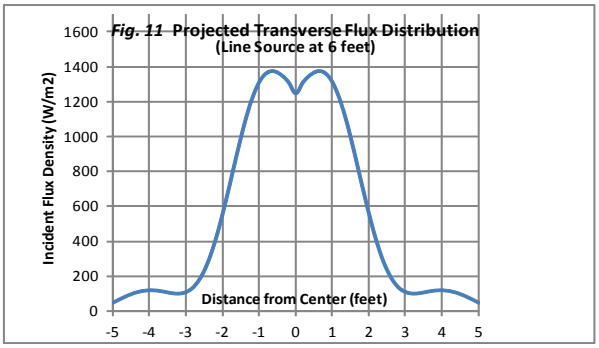

Formulas:

I = -ATAN((C-G)/(D-B))

J = I*180/3.1416

K = ((C-G)^2+(D-B)^2)^0.5

L = -E*3.1416/180+I

M =L*180/3.1416

N = (16*(COS(L))^16-2.9*COS(15*L)/((((L*57.3)^2)^0.5+1)^(1/5)))/13.1

O = 6*F38*N38*COS(I38)*2.93/(k38^1.6)

D12 = AVERAGE(C12:C62)

F12 = C12/1370

G12 = D12/1370

Macro:

```
Sub CERST001A3A()
Dim i As Long

For i = 12 To 62
Cells(4, 7) = Cells(i, 2)
Calculate
Cells(i, 3) = Cells(9, 16)
Next i
End Sub
```

Spreadsheet C.5

Column A

↓

CREST003A-1

BOTTOM 05/27/2011 10/18/2011

Bar	XS(ft)	YS(ft)	XT	B(deg)	EO(W/m2)	YT	A(rad)	A(deg)	S(ft)	G(rad)	G(deg)	D	ET(W/m2)
1.000	0.000	-5.000	6.000	0.000	1247.0	5.200	1.039	59.534	11.834	1.039	59.534	0.097	20.63
2.000	0.000	-4.000	6.000	0.000	1247.0	5.200	0.993	56.889	10.984	0.993	56.889	0.068	17.48
3.000	0.000	-2.500	6.000	0.000	1247.0	5.200	0.909	52.073	9.762	0.909	52.073	-0.048	-16.83
4.000	0.000	-1.000	6.000	0.000	1247.0	5.200	0.802	45.939	8.628	0.802	45.939	-0.084	-40.88
5.000	0.000	1.000	6.000	0.000	1247.0	5.200	0.611	34.992	7.324	0.611	34.992	0.155	114.83
6.000	0.000	2.500	6.000	0.000	1247.0	5.200	0.423	24.228	6.580	0.423	24.228	0.163	160.41
7.000	0.000	4.000	6.000	0.000	1247.0	5.200	0.197	11.310	6.119	0.197	11.310	1.024	1213.69
8.000	0.000	5.000	6.000	0.000	1247.0	5.200	0.033	1.909	6.003	0.033	1.909	1.054	1311.93

ET Sum: 2781.26

YT Values	ET Sum	ET Average	Pct. Dev.	IR Suns	Avg. IR Suns
-5.200	2781.26	3461.57	-19.7	2.030	2.527
-5.000	2888.05	3461.57	-16.6	2.108	2.527
-4.800	3109.79	3461.57	-10.2	2.270	2.527
-4.600	3296.70	3461.57	-4.8	2.406	2.527
-4.400	3460.20	3461.57	0.0	2.526	2.527
-4.200	3593.23	3461.57	3.8	2.623	2.527
-4.000	3671.41	3461.57	6.1	2.680	2.527
-3.800	3835.10	3461.57	10.8	2.799	2.527
-3.600	3926.78	3461.57	13.4	2.866	2.527
-3.400	3958.34	3461.57	14.4	2.889	2.527
-3.200	3933.73	3461.57	13.6	2.871	2.527
-3.000	3862.60	3461.57	11.6	2.819	2.527
-2.800	3758.72	3461.57	8.6	2.744	2.527
-2.600	3632.36	3461.57	4.9	2.651	2.527
-2.400	3551.13	3461.57	2.6	2.592	2.527
-2.200	3518.52	3461.57	1.6	2.568	2.527
-2.000	3474.94	3461.57	0.4	2.536	2.527
-1.800	3420.89	3461.57	-1.2	2.497	2.527
-1.600	3356.18	3461.57	-3.0	2.450	2.527
-1.400	3285.64	3461.57	-5.1	2.398	2.527
-1.200	3217.14	3461.57	-7.1	2.348	2.527
-1.000	3144.02	3461.57	-9.2	2.295	2.527
-0.800	3219.44	3461.57	-7.0	2.350	2.527
-0.600	3288.65	3461.57	-5.0	2.400	2.527
-0.400	3354.55	3461.57	-3.1	2.449	2.527
-0.200	3402.65	3461.57	-1.7	2.484	2.527
0.000	3420.30	3461.57	-1.2	2.497	2.527
0.200	3402.65	3461.57	-1.7	2.484	2.527
0.400	3354.55	3461.57	-3.1	2.449	2.527
0.600	3288.65	3461.57	-5.0	2.400	2.527
0.800	3219.44	3461.57	-7.0	2.350	2.527
1.000	3144.02	3461.57	-9.2	2.295	2.527
1.200	3217.14	3461.57	-7.1	2.348	2.527
1.400	3285.64	3461.57	-5.1	2.398	2.527
1.600	3356.18	3461.57	-3.0	2.450	2.527
1.800	3420.89	3461.57	-1.2	2.497	2.527
2.000	3474.94	3461.57	0.4	2.536	2.527
2.200	3518.52	3461.57	1.6	2.568	2.527
2.400	3551.13	3461.57	2.6	2.592	2.527
2.600	3632.36	3461.57	4.9	2.651	2.527
2.800	3758.72	3461.57	8.6	2.744	2.527
3.000	3862.60	3461.57	11.6	2.819	2.527
3.200	3933.73	3461.57	13.6	2.871	2.527
3.400	3958.34	3461.57	14.4	2.889	2.527
3.600	3926.78	3461.57	13.4	2.866	2.527
3.800	3835.10	3461.57	10.8	2.799	2.527
4.000	3671.41	3461.57	6.1	2.680	2.527
4.200	3593.23	3461.57	3.8	2.623	2.527
4.400	3460.20	3461.57	0.0	2.526	2.527
4.600	3296.70	3461.57	-4.8	2.406	2.527
4.800	3109.79	3461.57	-10.2	2.270	2.527
5.000	2888.05	3461.57	-16.6	2.108	2.527
5.200	2781.26	3461.57	-19.7	2.030	2.527

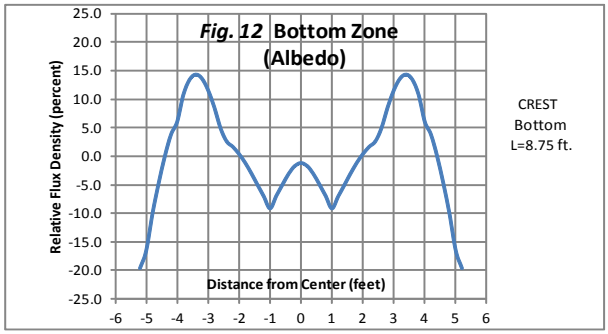

Formulas:

I = -ATAN((C-G)/(D-B))

J = I*180/3.1416

K = ((C-G)^2+(D-B)^2)^0.5

L = -E*3.1416/180+I

M =L*180/3.1416

N = (16*(COS(L))^16-2.9*COS(15*L)/((((L*57.3)^2)^0.5+1)^(1/5)))/13.1

O = 6*F*N*COS(I)*2.93/(K^1.6)

D15 = AVERAGE(C15:C39)

E15 = (C15-D15)/D15*100

F15 = C15/1370

G15 = D15/1370

Macro:

```
Sub CERST003AM()
Dim i As Long

For i = 15 To 67
Cells(4, 7) = Cells(i, 2)
Calculate
Cells(i, 3) = Cells(13, 16)
Next i
End Sub
```

Spreadsheet C.6

Column A

↓

CREST003A0

BOTTOM 05/27/2011 10/18/2011

Bar	XS(ft)	YS(ft)	XT	B(deg)	EO(W/m2)	YT	A(rad)	A(deg)	S(ft)	G(rad)	G(deg)	D	ET(W/m2)
1.000	0.000	-5.000	6.000	-10.000	1247.0	5.200	1.039	59.534	11.834	1.214	69.534	-0.075	-16.10
2.000	0.000	-4.000	6.000	-3.000	1247.0	5.200	0.993	56.889	10.984	1.045	59.889	0.097	25.19
3.000	0.000	-2.500	6.000	0.000	1247.0	5.200	0.909	52.073	9.762	0.909	52.073	-0.048	-16.83
4.000	0.000	-1.000	6.000	2.000	1247.0	5.200	0.802	45.939	8.628	0.767	43.939	-0.044	-21.29
5.000	0.000	1.000	6.000	-2.000	1247.0	5.200	0.611	34.992	7.324	0.646	36.992	0.137	101.63
6.000	0.000	2.500	6.000	0.000	1247.0	5.200	0.423	24.228	6.580	0.423	24.228	0.163	160.41
7.000	0.000	4.000	6.000	3.000	1247.0	5.200	0.197	11.310	6.119	0.145	8.310	1.112	1317.84
8.000	0.000	5.000	6.000	10.000	1247.0	5.200	0.033	1.909	6.003	-0.141	-8.091	1.115	1388.10

ET Sum: 2938.95

YT Values	ET Sum	ET Average	Pct. Dev.	IR Suns	Avg. IR Suns
-5.200	2938.95	3140.20	-6.4	2.145	2.292
-5.000	3015.91	3140.20	-4.0	2.201	2.292
-4.800	3034.92	3140.20	-3.4	2.215	2.292
-4.600	3009.62	3140.20	-4.2	2.197	2.292
-4.400	2954.92	3140.20	-5.9	2.157	2.292
-4.200	2957.03	3140.20	-5.8	2.158	2.292
-4.000	3007.65	3140.20	-4.2	2.195	2.292
-3.800	3059.79	3140.20	-2.6	2.233	2.292
-3.600	3108.57	3140.20	-1.0	2.269	2.292
-3.400	3143.53	3140.20	0.1	2.295	2.292
-3.200	3157.59	3140.20	0.6	2.305	2.292
-3.000	3150.85	3140.20	0.3	2.300	2.292
-2.800	3129.82	3140.20	-0.3	2.285	2.292
-2.600	3099.90	3140.20	-1.3	2.263	2.292
-2.400	3125.07	3140.20	-0.5	2.281	2.292
-2.200	3204.63	3140.20	2.1	2.339	2.292
-2.000	3272.99	3140.20	4.2	2.389	2.292
-1.800	3322.45	3140.20	5.8	2.425	2.292
-1.600	3343.52	3140.20	6.5	2.441	2.292
-1.400	3332.89	3140.20	6.1	2.433	2.292
-1.200	3295.01	3140.20	4.9	2.405	2.292
-1.000	3238.67	3140.20	3.1	2.364	2.292
-0.800	3160.70	3140.20	0.7	2.307	2.292
-0.600	3204.16	3140.20	2.0	2.339	2.292
-0.400	3235.79	3140.20	3.0	2.362	2.292
-0.200	3258.06	3140.20	3.8	2.378	2.292
0.000	3266.30	3140.20	4.0	2.384	2.292
0.200	3258.06	3140.20	3.8	2.378	2.292
0.400	3235.79	3140.20	3.0	2.362	2.292
0.600	3204.16	3140.20	2.0	2.339	2.292
0.800	3160.70	3140.20	0.7	2.307	2.292
1.000	3238.67	3140.20	3.1	2.364	2.292
1.200	3295.01	3140.20	4.9	2.405	2.292
1.400	3332.89	3140.20	6.1	2.433	2.292
1.600	3343.52	3140.20	6.5	2.441	2.292
1.800	3322.45	3140.20	5.8	2.425	2.292
2.000	3272.99	3140.20	4.2	2.389	2.292
2.200	3204.63	3140.20	2.1	2.339	2.292
2.400	3125.07	3140.20	-0.5	2.281	2.292
2.600	3099.90	3140.20	-1.3	2.263	2.292
2.800	3129.82	3140.20	-0.3	2.285	2.292
3.000	3150.85	3140.20	0.3	2.300	2.292
3.200	3157.59	3140.20	0.6	2.305	2.292
3.400	3143.53	3140.20	0.1	2.295	2.292
3.600	3108.57	3140.20	-1.0	2.269	2.292
3.800	3059.79	3140.20	-2.6	2.233	2.292
4.000	3007.65	3140.20	-4.2	2.195	2.292
4.200	2957.03	3140.20	-5.8	2.158	2.292
4.400	2954.92	3140.20	-5.9	2.157	2.292
4.600	3009.62	3140.20	-4.2	2.197	2.292
4.800	3034.92	3140.20	-3.4	2.215	2.292
5.000	3015.91	3140.20	-4.0	2.201	2.292
5.200	2938.95	3140.20	-6.4	2.145	2.292

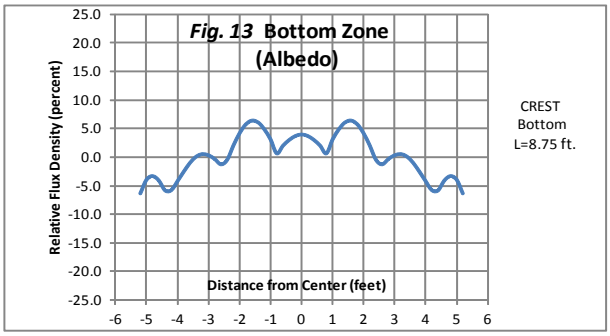

Formulas:

I = -ATAN((C-G)/(D-B))

J = I*180/3.1416

K = ((C-G)^2+(D-B)^2)^0.5

L = -E*3.1416/180+I

M =L*180/3.1416

N = (16*(COS(L))^16-2.9*COS(15*L)/((((L*57.3)^2)^0.5+1)^(1/5)))/13.1

O = 6*F*N*COS(I)*2.93/(K^1.6)

D15 = AVERAGE(C15:C39)

E15 = (C15-D15)/D15*100

F15 = C15/1370

G15 = D15/1370

Macro:

```
Sub CERST003AM()
Dim i As Long

For i = 15 To 67
Cells(4, 7) = Cells(i, 2)
Calculate
Cells(i, 3) = Cells(13, 16)
Next i
End Sub
```

Spreadsheet C.7

Column A

↓

CREST003A

BOTTOM 05/27/2011 06/14/2011

Bar	XS(ft)	YS(ft)	XT	B(deg)	EO(W/m2)	YT	A(rad)	A(deg)	S(ft)	G(rad)	G(deg)	D	ET(W/m2)
1.000	0.000	-5.000	6.000	-10.000	1247.0	5.200	1.039	59.534	11.834	1.214	69.534	-0.075	-16.10
2.000	0.000	-4.000	6.000	-3.000	1247.0	5.200	0.993	56.889	10.984	1.045	59.889	0.097	25.19
3.000	0.000	-2.500	6.000	0.000	1122.3	5.200	0.909	52.073	9.762	0.909	52.073	-0.048	-15.14
4.000	0.000	-1.000	6.000	2.000	1122.3	5.200	0.802	45.939	8.628	0.767	43.939	-0.044	-19.16
5.000	0.000	1.000	6.000	-2.000	1122.3	5.200	0.611	34.992	7.324	0.646	36.992	0.137	91.47
6.000	0.000	2.500	6.000	0.000	1122.3	5.200	0.423	24.228	6.580	0.423	24.228	0.163	144.37
7.000	0.000	4.000	6.000	3.000	1247.0	5.200	0.197	11.310	6.119	0.145	8.310	1.112	1317.84
8.000	0.000	5.000	6.000	10.000	1247.0	5.200	0.033	1.909	6.003	-0.141	-8.091	1.115	1388.10

ET Sum: 2916.56

YT Values	ET Sum	ET Average	Pct. Dev.	IR Suns	Avg. IR Suns
-5.200	2916.56	2942.93	-0.9	2.129	2.148
-5.000	2984.29	2942.93	1.4	2.178	2.148
-4.800	2991.06	2942.93	1.6	2.183	2.148
-4.600	2950.72	2942.93	0.3	2.154	2.148
-4.400	2878.77	2942.93	-2.2	2.101	2.148
-4.200	2862.41	2942.93	-2.7	2.089	2.148
-4.000	2894.49	2942.93	-1.6	2.113	2.148
-3.800	2929.08	2942.93	-0.5	2.138	2.148
-3.600	2961.96	2942.93	0.6	2.162	2.148
-3.400	2982.77	2942.93	1.4	2.177	2.148
-3.200	2983.91	2942.93	1.4	2.178	2.148
-3.000	2964.47	2942.93	0.7	2.164	2.148
-2.800	2929.99	2942.93	-0.4	2.139	2.148
-2.600	2885.74	2942.93	-1.9	2.106	2.148
-2.400	2890.27	2942.93	-1.8	2.110	2.148
-2.200	2944.28	2942.93	0.0	2.149	2.148
-2.000	2989.96	2942.93	1.6	2.182	2.148
-1.800	3021.32	2942.93	2.7	2.205	2.148
-1.600	3030.30	2942.93	3.0	2.212	2.148
-1.400	3013.95	2942.93	2.4	2.200	2.148
-1.200	2975.89	2942.93	1.1	2.172	2.148
-1.000	2923.43	2942.93	-0.7	2.134	2.148
-0.800	2853.00	2942.93	-3.1	2.082	2.148
-0.600	2892.68	2942.93	-1.7	2.111	2.148
-0.400	2921.96	2942.93	-0.7	2.133	2.148
-0.200	2942.67	2942.93	0.0	2.148	2.148
0.000	2950.34	2942.93	0.3	2.154	2.148
0.200	2942.67	2942.93	0.0	2.148	2.148
0.400	2921.96	2942.93	-0.7	2.133	2.148
0.600	2892.68	2942.93	-1.7	2.111	2.148
0.800	2853.00	2942.93	-3.1	2.082	2.148
1.000	2923.43	2942.93	-0.7	2.134	2.148
1.200	2975.89	2942.93	1.1	2.172	2.148
1.400	3013.95	2942.93	2.4	2.200	2.148
1.600	3030.30	2942.93	3.0	2.212	2.148
1.800	3021.32	2942.93	2.7	2.205	2.148
2.000	2989.96	2942.93	1.6	2.182	2.148
2.200	2944.28	2942.93	0.0	2.149	2.148
2.400	2890.27	2942.93	-1.8	2.110	2.148
2.600	2885.74	2942.93	-1.9	2.106	2.148
2.800	2929.99	2942.93	-0.4	2.139	2.148
3.000	2964.47	2942.93	0.7	2.164	2.148
3.200	2983.91	2942.93	1.4	2.178	2.148
3.400	2982.77	2942.93	1.4	2.177	2.148
3.600	2961.96	2942.93	0.6	2.162	2.148
3.800	2929.08	2942.93	-0.5	2.138	2.148
4.000	2894.49	2942.93	-1.6	2.113	2.148
4.200	2862.41	2942.93	-2.7	2.089	2.148
4.400	2878.77	2942.93	-2.2	2.101	2.148
4.600	2950.72	2942.93	0.3	2.154	2.148
4.800	2991.06	2942.93	1.6	2.183	2.148
5.000	2984.29	2942.93	1.4	2.178	2.148
5.200	2916.56	2942.93	-0.9	2.129	2.148

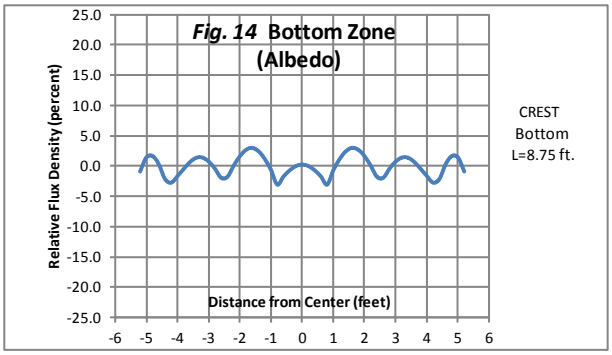

Formulas:

I = -ATAN((C-G)/(D-B))

J = I*180/3.1416

K = ((C-G)^2+(D-B)^2)^0.5

L = -E*3.1416/180+I

M =L*180/3.1416

N = (16*(COS(L))^16-2.9*COS(15*L)/((((L*57.3)^2)^0.5+1)^(1/5)))/13.1

O = 6*F*N*COS(I)*2.93/(K^1.6)

D15 = AVERAGE(C15:C39)

E15 = (C15-D15)/D15*100

F15 = C15/1370

G15 = D15/1370

Macro:

```
Sub CERST003AM()
Dim i As Long

For i = 15 To 67
Cells(4, 7) = Cells(i, 2)
Calculate
Cells(i, 3) = Cells(13, 16)
Next i
End Sub
```

Spreadsheet C.8

Column A

↓

CREST003A2

BOTTOM 05/27/2011 06/14/2011

Bar	XS(ft)	YS(ft)	XT	B(deg)	EO E0(W/m2)	YT	A(rad)	A(deg)	S(ft)	G(rad)	G(deg)	D	ET(W/m2)
1.000	0.000	-5.000	6.000	-10.000	1247.0	5.200	1.039	59.534	11.834	1.214	69.534	-0.075	-16.10
2.000	0.000	-4.000	6.000	-3.000	1247.0	5.200	0.993	56.889	10.984	1.045	59.889	0.097	25.19
3.000	0.000	-2.500	6.000	0.000	1122.3	5.200	0.909	52.073	9.762	0.909	52.073	-0.048	-15.14
4.000	0.000	-1.000	6.000	2.000	1122.3	5.200	0.802	45.939	8.628	0.767	43.939	-0.044	-19.16
5.000	0.000	1.000	6.000	-2.000	1122.3	5.200	0.611	34.992	7.324	0.646	36.992	0.137	91.47
6.000	0.000	2.500	6.000	0.000	1122.3	5.200	0.423	24.228	6.580	0.423	24.228	0.163	144.37
7.000	0.000	4.000	6.000	3.000	1247.0	5.200	0.197	11.310	6.119	0.145	8.310	1.112	1317.84
8.000	0.000	5.000	6.000	10.000	1247.0	5.200	0.033	1.909	6.003	-0.141	-8.091	1.115	1388.10

YT Values	ET1	ET2	ET3	ET4	ET5	ET6	ET7	ET8
-5.200	1388.1	1317.8	144.4	91.5	-19.2	-15.1	25.2	-16.1
-5.000	1340.1	1348.7	209.0	105.2	-8.5	-21.0	25.8	-15.0
-4.800	1238.9	1345.0	304.3	112.5	4.6	-26.7	25.9	-13.4
-4.600	1089.1	1317.7	429.2	113.1	19.8	-31.9	25.1	-11.3
-4.400	905.1	1273.7	577.3	107.8	36.4	-36.2	23.5	-8.8
-4.200	707.5	1288.2	737.5	99.7	53.4	-39.0	20.9	-5.7
-4.000	518.9	1342.0	895.0	93.9	69.5	-40.0	17.3	-2.1
-3.800	358.6	1379.5	1034.0	97.5	83.5	-38.5	12.5	2.0
-3.600	238.9	1390.3	1141.4	118.6	93.8	-34.3	6.6	6.5
-3.400	163.4	1361.4	1209.0	165.0	99.7	-26.9	-0.3	11.4
-3.200	127.6	1284.7	1236.4	242.3	100.5	-16.2	-8.0	16.5
-3.000	121.0	1160.8	1230.1	352.6	97.0	-2.3	-16.4	21.7
-2.800	130.8	999.1	1200.9	492.3	91.0	14.3	-25.1	26.7
-2.600	144.5	815.9	1156.7	652.1	85.7	32.9	-33.4	31.3
-2.400	152.5	630.4	1156.7	818.0	86.2	52.2	-41.0	35.2
-2.200	149.2	460.8	1200.9	973.1	98.3	70.9	-46.9	38.0
-2.000	133.1	320.7	1230.1	1101.6	128.6	87.1	-50.5	39.3
-1.800	106.0	217.2	1236.4	1191.7	182.9	99.2	-50.8	38.8
-1.600	71.7	150.8	1209.0	1238.9	265.0	106.0	-47.2	36.1
-1.400	34.9	116.6	1141.4	1246.7	375.5	106.9	-39.1	31.0
-1.200	0.2	106.4	1034.0	1224.7	510.6	102.7	-26.0	23.3
-1.000	-29.0	110.4	895.0	1184.7	661.9	95.7	-8.3	13.1
-0.800	-50.4	119.9	737.5	1124.9	816.9	90.0	13.6	0.5
-0.600	-63.1	127.7	577.3	1173.3	961.3	91.5	38.4	-13.7
-0.400	-67.4	129.5	429.2	1206.9	1081.2	107.2	64.2	-28.7
-0.200	-64.4	123.2	304.3	1223.5	1166.4	144.4	88.6	-43.3
0.000	-55.7	109.1	209.0	1212.8	1212.8	209.0	109.1	-55.7
0.200	-43.3	88.6	144.4	1166.4	1223.5	304.3	123.2	-64.4
0.400	-28.7	64.2	107.2	1081.2	1206.9	429.2	129.5	-67.4
0.600	-13.7	38.4	91.5	961.3	1173.3	577.3	127.7	-63.1
0.800	0.5	13.6	90.0	816.9	1124.9	737.5	119.9	-50.4
1.000	13.1	-8.3	95.7	661.9	1184.7	895.0	110.4	-29.0
1.200	23.3	-26.0	102.7	510.6	1224.7	1034.0	106.4	0.2
1.400	31.0	-39.1	106.9	375.5	1246.7	1141.4	116.6	34.9
1.600	36.1	-47.2	106.0	265.0	1238.9	1209.0	150.8	71.7
1.800	38.8	-50.8	99.2	182.9	1191.7	1236.4	217.2	106.0
2.000	39.3	-50.5	87.1	128.6	1101.6	1230.1	320.7	133.1
2.200	38.0	-46.9	70.9	98.3	973.1	1200.9	460.8	149.2
2.400	35.2	-41.0	52.2	86.2	818.0	1156.7	630.4	152.5
2.600	31.3	-33.4	32.9	85.7	652.1	1156.7	815.9	144.5
2.800	26.7	-25.1	14.3	91.0	492.3	1200.9	999.1	130.8
3.000	21.7	-16.4	-2.3	97.0	352.6	1230.1	1160.8	121.0
3.200	16.5	-8.0	-16.2	100.5	242.3	1236.4	1284.7	127.6
3.400	11.4	-0.3	-26.9	99.7	165.0	1209.0	1361.4	163.4
3.600	6.5	6.6	-34.3	93.8	118.6	1141.4	1390.3	238.9
3.800	2.0	12.5	-38.5	83.5	97.5	1034.0	1379.5	358.6
4.000	-2.1	17.3	-40.0	69.5	93.9	895.0	1342.0	518.9
4.200	-5.7	20.9	-39.0	53.4	99.7	737.5	1288.2	707.5
4.400	-8.8	23.5	-36.2	36.4	107.8	577.3	1273.7	905.1
4.600	-11.3	25.1	-31.9	19.8	113.1	429.2	1317.7	1089.1
4.800	-13.4	25.9	-26.7	4.6	112.5	304.3	1345.0	1238.9
5.000	-15.0	25.8	-21.0	-8.5	105.2	209.0	1348.7	1340.1
5.200	-16.1	25.2	-15.1	-19.2	91.5	144.4	1317.8	1388.1

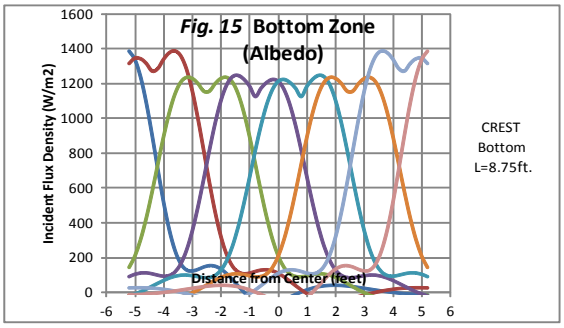

Formulas:

I = -ATAN((C-G)/(D-B))

J = I*180/3.1416

K = ((C-G)^2+(D-B)^2)^0.5

L = -E*3.1416/180+I

M =L*180/3.1416

N = (16*(COS(L))^16-2.9*COS(15*L)/((((L*57.3)^2)^0.5+1)^(1/5)))/13.1

O = 6*F*N*COS(I)*2.93/(K^1.6)

D15 = AVERAGE(C15:C67)

E15 = (C15-D15)/D15*100

F15 = C15/1370

G15 = D15/1370

Macro:

```
Sub CERST003A2M()
Dim i As Long

For i = 15 To 67
Cells(4, 7) = Cells(i, 2)
Calculate
Cells(i.3) = Cells(4,15)
Cells(i.4) = Cells(5,15)
Cells(i.5) = Cells(6,15)
Cells(i.6) = Cells(7,15)
Cells(i.7) = Cells(8,15)
Cells(i.8) = Cells(9,15)
Cells(i.9) = Cells(10,15)
Cells(i.10) = Cells(11,15)
Next i
End Sub
```

Spreadsheet C.9

Column A

↓

CREST002A

TOP 05/27/2011 06/14/2011

Bar	XS(ft)	YS(ft)	XT	B(deg)	EO(W/m2)	YT	A(rad)	A(deg)	S(ft)	G(rad)	G(deg)	D	ET(W/m2)
1.000	0.000	-4.500	8.000	-12.500	1247.0	5.200	0.881	50.486	12.573	1.099	62.986	0.068	16.61
2.000	0.000	-3.250	8.000	-3.000	997.6	5.200	0.813	46.567	11.636	0.865	49.567	-0.091	-21.73
3.000	0.000	-1.500	8.000	1.000	1159.7	5.200	0.697	39.946	10.435	0.680	38.946	0.098	35.87
4.000	0.000	1.500	8.000	-1.000	1159.7	5.200	0.433	24.820	8.814	0.451	25.820	0.125	71.16
5.000	0.000	3.250	8.000	3.000	997.6	5.200	0.239	13.699	8.234	0.187	10.699	1.050	613.33
6.000	0.000	4.500	8.000	12.500	1247.0	5.200	0.087	5.001	8.031	-0.131	-7.499	1.120	872.46

ET Sum: 1587.70

YT Values	ET Sum	ET Average	Pct. Dev.	IR Suns	Avg. IR Suns
-5.200	1587.70	1637.64	-3.0	1.159	1.195
-5.000	1638.74	1637.64	0.1	1.196	1.195
-4.800	1669.29	1637.64	1.9	1.218	1.195
-4.600	1679.70	1637.64	2.6	1.226	1.195
-4.400	1672.71	1637.64	2.1	1.221	1.195
-4.200	1652.94	1637.64	0.9	1.207	1.195
-4.000	1625.75	1637.64	-0.7	1.187	1.195
-3.800	1595.01	1637.64	-2.6	1.164	1.195
-3.600	1579.55	1637.64	-3.5	1.153	1.195
-3.400	1599.07	1637.64	-2.4	1.167	1.195
-3.200	1619.73	1637.64	-1.1	1.182	1.195
-3.000	1642.00	1637.64	0.3	1.199	1.195
-2.800	1662.51	1637.64	1.5	1.214	1.195
-2.600	1677.25	1637.64	2.4	1.224	1.195
-2.400	1682.98	1637.64	2.8	1.228	1.195
-2.200	1678.09	1637.64	2.5	1.225	1.195
-2.000	1662.97	1637.64	1.5	1.214	1.195
-1.800	1639.70	1637.64	0.1	1.197	1.195
-1.600	1610.91	1637.64	-1.6	1.176	1.195
-1.400	1575.40	1637.64	-3.8	1.150	1.195
-1.200	1587.14	1637.64	-3.1	1.158	1.195
-1.000	1606.68	1637.64	-1.9	1.173	1.195
-0.800	1626.62	1637.64	-0.7	1.187	1.195
-0.600	1646.44	1637.64	0.5	1.202	1.195
-0.400	1663.57	1637.64	1.6	1.214	1.195
-0.200	1675.24	1637.64	2.3	1.223	1.195
0.000	1679.38	1637.64	2.5	1.226	1.195
0.200	1675.24	1637.64	2.3	1.223	1.195
0.400	1663.57	1637.64	1.6	1.214	1.195
0.600	1646.44	1637.64	0.5	1.202	1.195
0.800	1626.62	1637.64	-0.7	1.187	1.195
1.000	1606.68	1637.64	-1.9	1.173	1.195
1.200	1587.14	1637.64	-3.1	1.158	1.195
1.400	1575.40	1637.64	-3.8	1.150	1.195
1.600	1610.91	1637.64	-1.6	1.176	1.195
1.800	1639.70	1637.64	0.1	1.197	1.195
2.000	1662.97	1637.64	1.5	1.214	1.195
2.200	1678.09	1637.64	2.5	1.225	1.195
2.400	1682.98	1637.64	2.8	1.228	1.195
2.600	1677.25	1637.64	2.4	1.224	1.195
2.800	1662.51	1637.64	1.5	1.214	1.195
3.000	1642.00	1637.64	0.3	1.199	1.195
3.200	1619.73	1637.64	-1.1	1.182	1.195
3.400	1599.07	1637.64	-2.4	1.167	1.195
3.600	1579.55	1637.64	-3.5	1.153	1.195
3.800	1595.01	1637.64	-2.6	1.164	1.195
4.000	1625.75	1637.64	-0.7	1.187	1.195
4.200	1652.94	1637.64	0.9	1.207	1.195
4.400	1672.71	1637.64	2.1	1.221	1.195
4.600	1679.70	1637.64	2.6	1.226	1.195
4.800	1669.29	1637.64	1.9	1.218	1.195
5.000	1638.74	1637.64	0.1	1.196	1.195
5.200	1587.70	1637.64	-3.0	1.159	1.195

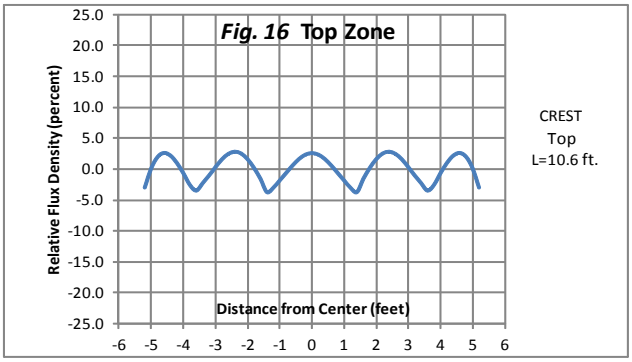

Formulas:

I = -ATAN((C-G)/(D-B))

J = I*180/3.1416

K = ((C-G)^2+(D-B)^2)^0.5

L = -E*3.1416/180+I

M =L*180/3.1416

N = (16*(COS(L))^16-2.9*COS(15*L)/((((L*57.3)^2)^0.5+1)^(1/5)))/13.1

O = 6*F*N*COS(I)*2.93/(K^1.6)

D15 = AVERAGE(C15:C67)

E15 = (C15-D15)/D15*100

F15 = C15/1370

G15 = D15/1370

Macro:

```
Sub CERST002AM()
Dim i As Long

For i = 15 To 67
Cells(4, 7) = Cells(i, 2)
Calculate
Cells(i, 3) = Cells(13, 16)
Next i
End Sub
```

Spreadsheet C.10

Column A

↓

CREST001F

UPPER FRONT W/REFLECTOR 05/27/2011 06/16/2011

Bar	XS(ft)	YS(ft)	XT	B(deg)	EO(W/m2)	YT	A(rad)	A(deg)	S(ft)	G(rad)	G(deg)	D	ET(W/m2)
1.000	0.000	-1.600	6.000	-3.000	623.5	2.400	0.588	33.690	7.211	0.640	36.690	0.141	54.53
2.000	0.000	-0.600	6.000	-3.000	623.5	2.400	0.464	26.565	6.708	0.516	29.565	0.118	55.22
3.000	0.000	1.000	6.000	3.000	1247.0	2.400	0.229	13.134	6.161	0.177	10.134	1.070	1245.85
4.000	0.000	2.000	6.000	3.000	1247.0	2.400	0.067	3.814	6.013	0.014	0.814	1.027	1273.66

ET Sum: 2629.26

YT Values	ET Sum	ET Average	Pct. Dev.	IR Suns	Avg. IR Suns
0.200	2618.29	2792.89	-6.3	1.911	2.039
0.400	2732.56	2792.89	-2.2	1.995	2.039
0.600	2814.36	2792.89	0.8	2.054	2.039
0.800	2861.92	2792.89	2.5	2.089	2.039
1.000	2876.29	2792.89	3.0	2.099	2.039
1.200	2856.47	2792.89	2.3	2.085	2.039
1.400	2850.61	2792.89	2.1	2.081	2.039
1.600	2876.55	2792.89	3.0	2.100	2.039
1.800	2863.75	2792.89	2.5	2.090	2.039
2.000	2813.76	2792.89	0.7	2.054	2.039
2.200	2720.82	2792.89	-2.6	1.986	2.039
2.400	2629.26	2792.89	-5.9	1.919	2.039

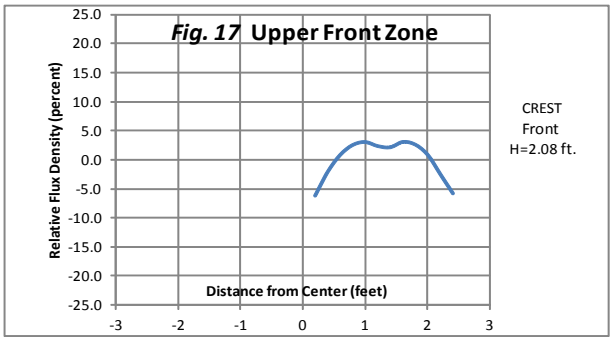

Formulas:

I = -ATAN((C-G)/(D-B))

J = I*180/3.1416

K = ((C-G)^2+(D-B)^2)^0.5

L = -E*3.1416/180+I

M =L*180/3.1416

N = (16*(COS(L))^16-2.9*COS(15*L)/((((L*57.3)^2)^0.5+1)^(1/5)))/13.1

O = 6*F*N*COS(I)*2.93/(K^1.6)

D15 = AVERAGE(C26:C37)

E15 = (C26-D26)/D26*100

F15 = C26/1370

G15 = D26/1370

Macro:

```
Sub CERST001FM()
Dim i As Long

For i = 26 To 37
Cells(4, 7) = Cells(i, 2)
Calculate
Cells(i, 3) = Cells(13, 16)
Next i
End Sub
```

EO (direct):

1500*0.286/0.344 = 1247 W/m2

EO (reflector image):

1247*0.5=623.5 W/m2

Spreadsheet C.11

Column A

↓

CREST001G

LOWER (RECESSED) FRONT W/REFLECTOR 05/27/2011 06/16/2011

Bar	XS(ft)	YS(ft)	XT	B(deg)	EO(W/m2)	YT	A(rad)	A(deg)	S(ft)	G(rad)	G(deg)	D	ET(W/m2)
1.000	0.000	-2.000	6.833	-1.500	1247.0	0.200	0.311	17.847	7.178	0.338	19.347	0.440	392.02
2.000	0.000	-1.000	6.833	-1.000	1247.0	0.200	0.174	9.961	6.938	0.191	10.961	1.040	1012.05
3.000	0.000	1.400	6.833	1.000	623.5	0.200	-0.174	-9.961	6.938	-0.191	-10.961	1.040	506.03
4.000	0.000	2.400	6.833	1.500	623.5	0.200	-0.311	-17.847	7.178	-0.338	-19.347	0.440	196.01

ET Sum: 2106.11

YT Values	ET Sum	ET Average	Pct. Dev.	IR Suns	Avg. IR Suns
-2.600	2098.66	2251.95	-6.8	1.532	1.644
-2.400	2160.33	2251.95	-4.1	1.577	1.644
-2.200	2180.27	2251.95	-3.2	1.591	1.644
-2.000	2253.85	2251.95	0.1	1.645	1.644
-1.800	2300.57	2251.95	2.2	1.679	1.644
-1.600	2322.73	2251.95	3.1	1.695	1.644
-1.400	2323.87	2251.95	3.2	1.696	1.644
-1.200	2301.71	2251.95	2.2	1.680	1.644
-1.000	2310.66	2251.95	2.6	1.687	1.644
-0.800	2331.09	2251.95	3.5	1.702	1.644
-0.600	2329.23	2251.95	3.4	1.700	1.644
-0.400	2306.07	2251.95	2.4	1.683	1.644
-0.200	2260.70	2251.95	0.4	1.650	1.644
0.000	2193.34	2251.95	-2.6	1.601	1.644
0.200	2106.11	2251.95	-6.5	1.537	1.644

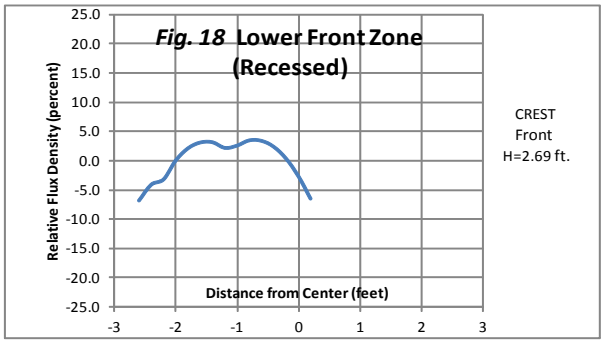

Formulas:

I = -ATAN((C-G)/(D-B))

J = I*180/3.1416

K = ((C-G)^2+(D-B)^2)^0.5

L = -E*3.1416/180+I

M =L*180/3.1416

N = (16*(COS(L))^16-2.9*COS(15*L)/((((L*57.3)^2)^0.5+1)^(1/5)))/13.1

O = 6*F*N*COS(I)*2.93/(K^1.6)

D15 = AVERAGE(C12:C26)

E15 = (C12-D12)/D12*100

F15 = C12/1370

G15 = D12/1370

Macro:

```
Sub CERST001GM()
Dim i As Long

For i = 12 To 26
Cells(4, 7) = Cells(i, 2)
Calculate
Cells(i, 3) = Cells(9, 16)
Next i
End Sub
```

EO (direct):

1500*0.286/0.344 = 1247 W/m2

EO (reflector image):

1247*0.5=623.5 W/m2

Spreadsheet C.12

Column A
↓

CREST003A4
PROJECTION BOTTOM 05/27/2011 06/14/2011

Bar	XS(ft)	YS(ft)	XT	B(deg)	E0(W/m2)	YT	A(rad)	A(deg)	S(ft)	G(rad)	G(deg)	D	ET(W/m2)
1.000	0.000	-5.000	8.500	-10.000	1247.0	5.300	0.881	50.469	13.354	1.055	60.469	0.096	21.27
2.000	0.000	-4.000	8.500	-3.000	1247.0	5.300	0.830	47.573	12.599	0.883	50.573	-0.078	-19.96
3.000	0.000	-2.500	8.500	0.000	1247.0	5.300	0.742	42.541	11.536	0.742	42.541	-0.005	-1.77
4.000	0.000	-1.000	8.500	2.000	0.0	5.300	0.638	36.545	10.580	0.603	34.545	0.155	0.00
5.000	0.000	1.000	8.500	-2.000	0.0	5.300	0.468	26.834	9.526	0.503	28.834	0.113	0.00
6.000	0.000	2.500	8.500	0.000	1247.0	5.300	0.318	18.232	8.949	0.318	18.232	0.528	329.98
7.000	0.000	4.000	8.500	3.000	1247.0	5.300	0.152	8.695	8.599	0.099	5.695	1.116	773.67
8.000	0.000	5.000	8.500	10.000	1247.0	5.300	0.035	2.021	8.505	-0.139	-7.979	1.116	795.75

YT Values	ET1	ET1 Refl. Correction	ET2	ET2 Shadow Correction	ET3	ET3 Shadow Correction	ET Sum	ET Average (bottom)	Pct. Dev.
-5.300	795.8	1.0	773.7	1.0	330.0	1.0	1899.4	2942.9	-35.5
-5.250	793.3	1.0	773.3	1.0	347.1	1.0	1913.7	2942.9	-35.0
-5.200	790.0	1.0	772.3	1.0	364.5	1.0	1926.8	2942.9	-34.5
-5.150	785.8	1.0	770.9	1.0	382.1	0.5	1747.8	2942.9	-40.6
-5.100	780.7	1.0	769.1	1.0	400.0	0.0	1549.8	2942.9	-47.3
-5.050	774.6	1.0	766.9	1.0	418.0	0.0	1541.5	2942.9	-47.6
-5.000	767.5	1.0	764.3	1.0	436.1	0.0	1531.8	2942.9	-47.9
-4.950	759.5	1.0	761.4	1.0	454.2	0.0	1520.9	2942.9	-48.3
-4.900	750.6	1.0	758.2	1.0	472.4	0.0	1508.7	2942.9	-48.7
-4.850	740.6	1.0	754.7	1.0	490.4	0.0	1495.3	2942.9	-49.2
-4.800	729.7	1.0	751.0	1.0	508.4	0.0	1480.7	2942.9	-49.7
-4.750	717.9	1.0	747.0	1.0	526.2	0.0	1465.0	2942.9	-50.2
-4.700	705.2	1.0	742.8	1.0	543.8	0.0	1448.0	2942.9	-50.8
-4.650	691.7	1.5	738.2	1.0	561.0	0.0	1775.7	2942.9	-39.7
-4.600	677.3	1.9	733.2	1.0	578.0	0.0	2020.0	2942.9	-31.4
-4.550	662.1	1.9	727.5	0.5	594.5	0.0	1621.7	2942.9	-44.9
-4.500	646.1	1.9	720.9	0.0	610.6	0.0	1227.6	2942.9	-58.3
-4.450	629.5	1.9	712.5	0.0	626.2	0.0	1196.0	2942.9	-59.4
-4.400	612.2	1.9	720.6	0.0	641.2	0.0	1163.2	2942.9	-60.5
4.400	612.2	1.9	720.6	0.0	641.2	0.0	1163.2	2942.9	-60.5
4.450	629.5	1.9	712.5	0.0	626.2	0.0	1196.0	2942.9	-59.4
4.500	646.1	1.9	720.9	0.0	610.6	0.0	1227.6	2942.9	-58.3
4.550	662.1	1.9	727.5	0.5	594.5	0.0	1621.7	2942.9	-44.9
4.600	677.3	1.9	733.2	1.0	578.0	0.0	2020.0	2942.9	-31.4
4.650	691.7	1.5	738.2	1.0	561.0	0.0	1775.7	2942.9	-39.7
4.700	705.2	1.0	742.8	1.0	543.8	0.0	1448.0	2942.9	-50.8
4.750	717.9	1.0	747.0	1.0	526.2	0.0	1465.0	2942.9	-50.2
4.800	729.7	1.0	751.0	1.0	508.4	0.0	1480.7	2942.9	-49.7
4.850	740.6	1.0	754.7	1.0	490.4	0.0	1495.3	2942.9	-49.2
4.900	750.6	1.0	758.2	1.0	472.4	0.0	1508.7	2942.9	-48.7
4.950	759.5	1.0	761.4	1.0	454.2	0.0	1520.9	2942.9	-48.3
5.000	767.5	1.0	764.3	1.0	436.1	0.0	1531.8	2942.9	-47.9
5.050	774.6	1.0	766.9	1.0	418.0	0.0	1541.5	2942.9	-47.6
5.100	780.7	1.0	769.1	1.0	400.0	0.0	1549.8	2942.9	-47.3
5.150	785.8	1.0	770.9	1.0	382.1	0.5	1747.8	2942.9	-40.6
5.200	790.0	1.0	772.3	1.0	364.5	1.0	1926.8	2942.9	-34.5
5.250	793.3	1.0	773.3	1.0	347.1	1.0	1913.7	2942.9	-35.0
5.300	795.8	1.0	773.7	1.0	330.0	1.0	1899.4	2942.9	-35.5

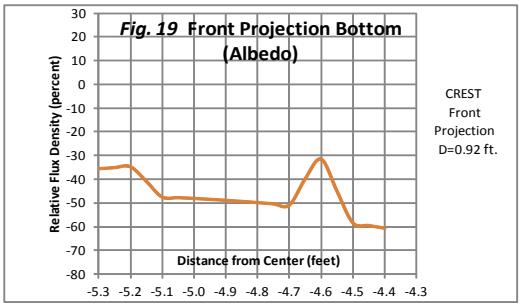

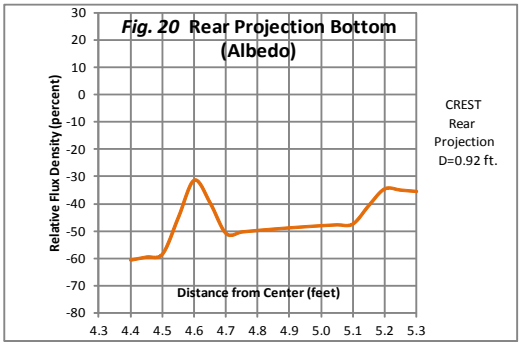

Formulas:
I = -ATAN((C-G)/(D-B))
J = I*180/3.1416
K = ((C-G)^2+(D-B)^2)^0.5
L = -E*3.1416/180+I
M =L*180/3.1416
N = (16*(COS(L))^16-2.9*COS(15*L)/((((L*57.3)^2)^0.5+1)^(1/5)))/13.1
O = 6*F*N*COS(I)*2.93/(K^1.6)

I15 = C15*D15+E15*F15+G15*H15
K15 = (IC15-J15)/J15*100

Macro:

```
Sub CERST003A4M()
Dim i As Long

For i = 15 To 31
Cells(4, 7) = Cells(i, 2)
Calculate
Cells(i, 3) = Cells(4, 15)
Cells(i, 5) = Cells(5, 15)
Cells(i, 7) = Cells(6, 15)
Next i

For i = 33 To 49
Cells(4, 7) = Cells(i, 2)
Calculate
Cells(i, 3) = Cells(11, 15)
Cells(i, 5) = Cells(10, 15)
Cells(i, 75) = Cells(9, 15)
Next i
End Sub
```

Spreadsheet C.13

Column A

↓

CREST001A3

REAR PROJECTION BOTTOM 05/27/2011 06/14/2011

Bar	EO(W/m2)	S(ft)	G(deg)	G(rad)	D	ET(W/m2)
1.000	1247.0	4.350	20.000	0.349	0.391	816.13

ET Sum: 816.13

G Values (degrees)	ETSum	ET Average	Pct. Dev.	IR Suns	Avg. IR Suns
-20.000	816.13	1880.36	-56.6	0.596	1.373
-18.000	1141.43	1880.36	-39.3	0.833	1.373
-16.000	1485.00	1880.36	-21.0	1.084	1.373
-14.000	1805.26	1880.36	-4.0	1.318	1.373
-12.000	2065.50	1880.36	9.8	1.508	1.373
-10.000	2241.79	1880.36	19.2	1.636	1.373
-8.000	2327.47	1880.36	23.8	1.699	1.373
-6.000	2333.36	1880.36	24.1	1.703	1.373
-4.000	2282.87	1880.36	21.4	1.666	1.373
-2.000	2201.98	1880.36	17.1	1.607	1.373
0.000	2085.94	1880.36	10.9	1.523	1.373
2.000	2201.98	1880.36	17.1	1.607	1.373
4.000	2282.87	1880.36	21.4	1.666	1.373
6.000	2333.36	1880.36	24.1	1.703	1.373
8.000	2327.47	1880.36	23.8	1.699	1.373
10.000	2241.79	1880.36	19.2	1.636	1.373
12.000	2065.50	1880.36	9.8	1.508	1.373
14.000	1805.26	1880.36	-4.0	1.318	1.373
16.000	1485.00	1880.36	-21.0	1.084	1.373
18.000	1141.43	1880.36	-39.3	0.833	1.373
20.000	816.13	1880.36	-56.6	0.596	1.373

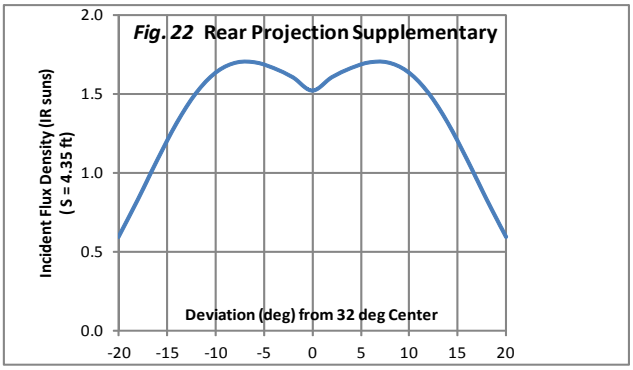

Formulas:
M = L*3.1416/180
N = (16*(COS(M))^16-2.9*COS(15*M)/((((M*57.3)^2)^0.5+1)^(1/5)))/13.1
O = 6*F*N*2.93/(K^1.6)

D = AVERAGE(C12:C32)
E = (C-D)/D*100
F = C/1370
G = D/1370

Macro:

```
Sub CERST001A3M()
Dim i As Long

For i = 12 To 32
Cells(4, 12) = Cells(i, 2)
Calculate
Cells(i, 3) = Cells(9, 16)
Next i
End Sub
```

Spreadsheet C.14

Column A
↓
CREST000
Table 2 CREST Illuminated Surfaces 04/04/2012

Table 2 Development of CREST In-Chamber Illumination Levels

Surface	Face Dimensions (ft. x ft.)	Required Flux Density (LEO suns)	Skin Material	Skin Thickness (mils)	ISA (div)	SSA (div)	SSA Correction Lg(%)	SSA Correction Xv(%)	CSSA (div)
Bottom	8.75 x 10.6	0.95	Slvr. Teflon	5	0.697	1.002	8.0	0.5	1.087
		0.65				0.685	8.0	0.5	0.744
Top	10.53 x 10.6	0.375	Alum. Mylar	4	1.488	0.844	8.0	2.5	0.933
Front Upper	2.09 x 10.6	0.927	Alum. Mylar	4	1.488	2.087	8.0	2.0	2.295
Front Lower	2.95 x 10.6	0.927	Slvr. Teflon	5	0.697	0.977	8.0	2.5	1.080
Rear	--	0.25	Alum. Mylar	4	1.488	0.563	8.0	-3.0	0.591
		0.5				1.126	8.0	-3.0	1.182
		0.75				1.688	8.0	-3.0	1.773

Formulas:

G12=F12*C12/0.661	J12=G12*(1+(H12+I12)/100)
G13=F12*C13/0.661	J13=G13*(1+(H13+I13)/100)
G15=F15*C15/0.661	J15=G15*(1+(H15+I15)/100)
G17=F17*C17/0.661	J17=G17*(1+(H17+I17)/100)
G19=F19*C19/0.661	J19=G19*(1+(H19+I19)/100)
G21=F21*C21/0.661	J21=G21*(1+(H21+I21)/100)
G22=F21*C22/0.661	J22=G22*(1+(H22+I22)/100)
G23=F21*C23/0.661	J13=G13*(1+(H23+I23)/100)

Spreadsheet C.15

Column A
↓
CREST000
Table 3 CREST In-Chamber Calibrated Levels 04/05/2012

Table 3 Development of CREST In-Chamber Power Control Levels

Surface	Original Illumination Source	Required Flux Density (LEO suns)	Skin Material	Master Channel	Hukseflux Reading (W/m2)	Correction CSSA/ICC	Auto Control Setpoint (W/m2)	Uncorrected Manual (percent)	Correction (CSSA/ ICC)^0.6	Corrected Manual (percent)
Bottom	Albedo	0.95	Slvr. Teflon	15	100	1.013	101.3	21	1.008	21.2
		0.65			52	1.000	52.0	17	1.000	17.0
Top	22 Deg. Sun	0.375	Alum. Mylar	12	191	0.979	187.0	36	0.987	35.5
Front Upper	22 Deg. Sun	0.927	Alum. Mylar	10	700	0.962	673.2	50	0.977	48.8
Front Lower	22 Deg. Sun	0.927	Slvr. Teflon	*11	none	none	none	24.5	1.017	24.9
Rear	Dark Side	0.25	Alum. Mylar	20	none	none	none	31	1.007	31.2
		0.5						51	1.011	51.6
		0.75						69	0.987	68.1

*Channel 11 command voltage slaved at 50.1 % of channel 10.

	CSSA/ICC		(CSSA/ICC)^0.6	
Formulas:	G12=1.09/1.076	H12=F12*G12	J12=(1.09/1.076)^0.6	K12=I12*J12
	G13=.74/.74	H12=F13*G13	J13=(0.74/0.74)^0.6	K13=I13*J13
	G15=.93/.95	H15=F15*G15	J15=(0.93/0.95)^0.6	K15=I15*J15
	G17=2.26/2.35	H17=F17*G17	J17=(2.26/2.35)^0.6	K17=I17*J17
			J19=(109.6/1.065)^0.6	K19=I19*J19
			J21=(0.59/0.583)^0.6	K21=I21*J21
			J22=(1.18/1.158)^0.6	K22=I22*J22
			J23=(1.77/1.81)^0.6	K23=I23*J23

Spreadsheet C.16

Column A

↓

CREST001E1

ARRAY BAR FALLOFF VS DISTANCE (S EXPONENT DEVELOPMENT) 06/06/2011 07/14/2011

Lamp	XS(ft)	YS(ft)	XT	EQ(W/m2)	YT	A(rad)	A(deg)	S(ft)	D	ET(W/m2)	ET Sum:
1.000	0.000	-5.625	13.000	1.000	0.000	0.408	23.398	14.165	0.918	0.004	0.083
2.000	0.000	-4.875	13.000	1.000	0.000	0.359	20.556	13.884	0.936	0.005	
3.000	0.000	-4.125	13.000	1.000	0.000	0.307	17.605	13.639	0.953	0.005	
4.000	0.000	-3.375	13.000	1.000	0.000	0.254	14.554	13.431	0.968	0.005	
5.000	0.000	-2.625	13.000	1.000	0.000	0.199	11.416	13.262	0.980	0.005	
6.000	0.000	-1.875	13.000	1.000	0.000	0.143	8.207	13.135	0.990	0.006	
7.000	0.000	-1.125	13.000	1.000	0.000	0.086	4.946	13.049	0.996	0.006	
8.000	0.000	-0.375	13.000	1.000	0.000	0.029	1.652	13.005	1.000	0.006	
9.000	0.000	0.375	13.000	1.000	0.000	-0.029	-1.652	13.005	1.000	0.006	
10.000	0.000	1.125	13.000	1.000	0.000	-0.086	-4.946	13.049	0.996	0.006	
11.000	0.000	1.875	13.000	1.000	0.000	-0.143	-8.207	13.135	0.990	0.006	
12.000	0.000	2.625	13.000	1.000	0.000	-0.199	-11.416	13.262	0.980	0.005	
13.000	0.000	3.375	13.000	1.000	0.000	-0.254	-14.554	13.431	0.968	0.005	
14.000	0.000	4.125	13.000	1.000	0.000	-0.307	-17.605	13.639	0.953	0.005	
15.000	0.000	4.875	13.000	1.000	0.000	-0.359	-20.556	13.884	0.936	0.005	
16.000	0.000	5.625	13.000	1.000	0.000	-0.408	-23.398	14.165	0.918	0.004	

XT-XS		ET Approximations					% Error				
Values	ET Sum	1/S	1/(S^1.6)	1/S^(MS+B)	1/(S^S^K)	1/(S^2)	1/S	1/(S^1.6)	1/S^(MS+B	1/(S^S^K)	1/(S^2)
6.000	0.286	0.286	0.286	0.286	0.286	0.286	0.074	0.069	0.074	0.143	-0.093
6.200	0.273	0.277	0.271	0.277	0.273	0.266	1.388	-0.593	1.330	-0.119	-2.701
6.400	0.261	0.268	0.258	0.268	0.260	0.248	2.733	-1.174	2.505	-0.346	-4.811
6.600	0.250	0.260	0.246	0.259	0.248	0.234	4.110	-1.682	3.599	-0.543	-6.459
6.800	0.239	0.252	0.234	0.250	0.237	0.220	5.516	-2.123	4.611	-0.712	-7.984
7.000	0.229	0.245	0.223	0.242	0.227	0.208	6.949	-2.504	5.543	-0.855	-9.399
7.200	0.220	0.238	0.214	0.234	0.218	0.196	8.410	-2.829	6.392	-0.975	-10.712
7.400	0.211	0.232	0.204	0.226	0.209	0.186	9.896	-3.103	7.161	-1.073	-11.935
7.600	0.203	0.226	0.196	0.219	0.200	0.176	11.406	-3.331	7.847	-1.152	-13.074
7.800	0.195	0.220	0.188	0.211	0.192	0.167	12.939	-3.516	8.454	-1.213	-14.138
8.000	0.187	0.215	0.180	0.204	0.185	0.159	14.494	-3.662	8.979	-1.258	-15.131
8.200	0.180	0.209	0.173	0.197	0.178	0.151	16.070	-3.773	9.425	-1.288	-16.062
8.400	0.174	0.204	0.167	0.191	0.171	0.144	17.666	-3.850	9.791	-1.305	-16.933
8.600	0.167	0.200	0.161	0.184	0.165	0.138	19.281	-3.896	10.079	-1.310	-17.751
8.800	0.161	0.195	0.155	0.178	0.159	0.131	20.914	-3.915	10.289	-1.304	-18.520
9.000	0.156	0.191	0.149	0.172	0.154	0.126	22.565	-3.908	10.423	-1.289	-19.243
9.200	0.150	0.187	0.144	0.166	0.148	0.120	24.233	-3.876	10.481	-1.265	-19.924
9.400	0.145	0.183	0.139	0.160	0.143	0.115	25.916	-3.823	10.466	-1.233	-20.566
9.600	0.140	0.179	0.135	0.155	0.138	0.110	27.614	-3.750	10.378	-1.194	-21.172
9.800	0.135	0.175	0.130	0.149	0.134	0.106	29.327	-3.657	10.219	-1.149	-21.744
10.000	0.131	0.172	0.126	0.144	0.129	0.102	31.053	-3.547	9.990	-1.099	-22.285
10.200	0.127	0.168	0.122	0.139	0.125	0.098	32.793	-3.421	9.694	-1.044	-22.798
10.400	0.123	0.165	0.119	0.134	0.121	0.094	34.546	-3.280	9.331	-0.985	-23.283
10.600	0.119	0.162	0.115	0.129	0.118	0.091	36.310	-3.125	8.904	-0.923	-23.743
10.800	0.115	0.159	0.112	0.125	0.114	0.087	38.086	-2.957	8.415	-0.857	-24.180
11.000	0.112	0.156	0.108	0.120	0.111	0.084	39.874	-2.777	7.866	-0.789	-24.595
11.200	0.108	0.153	0.105	0.116	0.107	0.081	41.672	-2.586	7.258	-0.719	-24.990
11.400	0.105	0.151	0.102	0.112	0.104	0.078	43.480	-2.385	6.594	-0.647	-25.365
11.600	0.102	0.148	0.100	0.108	0.101	0.076	45.298	-2.175	5.876	-0.573	-25.723
11.800	0.099	0.145	0.097	0.104	0.098	0.073	47.125	-1.955	5.106	-0.499	-26.063
12.000	0.096	0.143	0.094	0.100	0.096	0.071	48.962	-1.727	4.286	-0.424	-26.388
12.200	0.093	0.141	0.092	0.096	0.093	0.068	50.807	-1.492	3.418	-0.348	-26.698
12.400	0.091	0.138	0.090	0.093	0.090	0.066	52.660	-1.249	2.504	-0.272	-26.994
12.600	0.088	0.136	0.087	0.090	0.088	0.064	54.521	-1.000	1.548	-0.197	-27.277
12.800	0.086	0.134	0.085	0.086	0.086	0.062	56.391	-0.745	0.550	-0.121	-27.547
13.000	0.083	0.132	0.083	0.083	0.083	0.060	58.267	-0.484	-0.487	-0.046	-27.806

Upper Formulas:

```
J = -ATAN((C-H)/(E-B))
K = J*180/3.1416
L = ((C-H)^2+(E-B)^2)^0.5
O = COS(J)
P =G*O*COS(J)/L^2
Q = SUM(P4:P19)
```

Macro:

```
Sub CERST001EM()
Dim i As Long

For i = 25 To 60
Cells(5,5) = Cells(I,2)
Calculate
Cells(i,3) = Cells(5,17)
Next i
End Sub
```

Lower Formulas:

```
E = 6/B*0.286
F = 6*2.93/((B)^1.6)*0.286
G = (6/B)^(0.0857*B+0.486)*0.286
H = 6*1.496/((B)^(B^0.113))*0.286
I = 6*5.99/(B)^2)*0.286

K = (E-C)/C*100
L = (F-C)/C*100
M = (G-C)/C*100
N = (H-C)/C*100
O = (I-C)/C*100
```

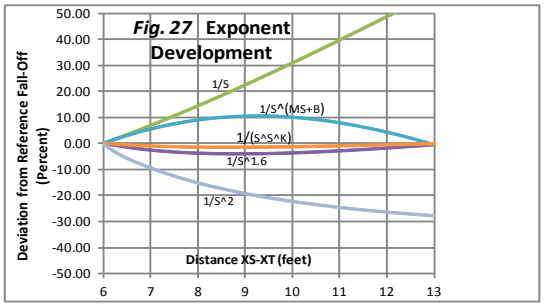

References

1. Pauls, Edward (Research Incorporated), "Energy Distribution Curve," *Acceptance Test Results for Thermal Simulator Test Fixture* (December 14, 1965): figures 2-2 and 2-5.
2. Ziemke, Robert, "Infrared Heater Used in Qualification Testing of International Space Station Radiators," NASA/TM—2004-212332 (2004): 12, figure 7a.
3. Ziemke, Robert, "Infrared Heater Used in Qualification Testing of International Space Station Radiators," NASA/TM—2004-212332 (2004): 7, step 5.
4. Henninger, John, "Solar Absorptance and Thermal Emittance of Some Spacecraft Thermal-Control Coatings," NASA Reference Publication 1121 (April 1984): 16.
5. Forsythe, W. E., and Worthing, A. G., "The Properties of Tungsten and the Characteristics of Tungsten Lamps," Astrophysical Journal, vol. 61 (1925): 171
6. Smith, Warren, "The Inverse Square Law," *Modern Optical engineering* (1966): 182.

Biography

Mr. Ziemke works in the Plum Brook Management Office at the NASA Glenn Research Center's Plum Brook station in Sandusky, Ohio. He is currently serving as an electronics engineer specializing in solar and thermal simulation, and analysis. He designed the infrared heating system for the qualification testing of the International Space Station radiators and has consulted on proposed design concepts for the *Orion* Crew Exploration Vehicle thermal simulation. In 1971, he designed the 7.2 megawatt SCR power control system for the Viking Centaur heated fairing jettison test performed at NASA Plum Brook's Space Power Facility. He has over 35 years experience as a NASA instrumentation and controls engineer. He holds a Bachelor's degree in electrical engineering from the Cleveland State University.

REPORT DOCUMENTATION PAGE	Form Approved OMB No. 0704-0188

1. REPORT DATE *(DD-MM-YYYY)*	2. REPORT TYPE	3. DATES COVERED *(From - To)*
01-03-2013	Technical Memorandum	

4. TITLE AND SUBTITLE
Solar Simulation for the CREST Preflight Thermal-Vacuum Test at B-2

5a. CONTRACT NUMBER

5b. GRANT NUMBER

5c. PROGRAM ELEMENT NUMBER

6. AUTHOR(S)
Ziemke, Robert, A.

5d. PROJECT NUMBER

5e. TASK NUMBER

5f. WORK UNIT NUMBER
WBS 750271.09.04.03

7. PERFORMING ORGANIZATION NAME(S) AND ADDRESS(ES)
National Aeronautics and Space Administration
John H. Glenn Research Center at Lewis Field
Cleveland, Ohio 44135-3191

8. PERFORMING ORGANIZATION REPORT NUMBER
E-18431

9. SPONSORING/MONITORING AGENCY NAME(S) AND ADDRESS(ES)
National Aeronautics and Space Administration
Washington, DC 20546-0001

10. SPONSORING/MONITOR'S ACRONYM(S)
NASA

11. SPONSORING/MONITORING REPORT NUMBER
NASA/TM-2013-217720

12. DISTRIBUTION/AVAILABILITY STATEMENT
Unclassified-Unlimited
Subject Categories: 14, 18, and 34
Available electronically at http://www.sti.nasa.gov
This publication is available from the NASA Center for AeroSpace Information, 443-757-5802

13. SUPPLEMENTARY NOTES

14. ABSTRACT
In June 2011, the multi-university sponsored Cosmic Ray Electron Synchrotron Telescope (CREST) has undergone thermal-vacuum qualification testing at the NASA Glenn Research Center (GRC), Plum Brook Station, Sandusky, Ohio. The testing was performed in the B-2 Space Propulsion Facility vacuum chamber. The CREST was later flown over the Antarctic region as the payload of a stratospheric balloon. Solar simulation was provided by a system of planar infrared lamp arrays specifically designed for CREST. The lamp arrays, in conjunction with a liquid-nitrogen-cooled cryoshroud, achieved the required thermal conditions for the qualification tests. This report focuses on the design and analysis of the planar arrays based on first principles. Computational spreadsheets are included in the report.

15. SUBJECT TERMS
Thermal vacuum tests; Infrared radiation; Luminaries; Flux density; Solar spectra; Pyranometers; Albedo

16. SECURITY CLASSIFICATION OF:			17. LIMITATION OF ABSTRACT	18. NUMBER OF PAGES	19a. NAME OF RESPONSIBLE PERSON
a. REPORT	b. ABSTRACT	c. THIS PAGE			STI Help Desk (email:help@sti.nasa.gov)
U	U	U	UU	46	19b. TELEPHONE NUMBER *(include area code)* 443-757-5802